

Index Pairs: from Dynamics to Combinatorics and Back

A Thesis
Presented to
The Faculty of the Division of Graduate Studies

by

Andrzej Szymczak

In Partial Fulfillment
of the Requirements for the Degree of
Doctor of Philosophy in Applied Mathematics

Georgia Institute of Technology
May 1999

Index Pairs: from Dynamics to Combinatorics and Back

Approved:

Konstantin Mischaikow, Chairman

George Cain

Luca Dieci

Robert Ghrist

Jarek Rossignac
College of Computing

Date Approved by Chairman _____

Contents

Symbolic Description of Dynamics via Index Pairs	1
Isolated Invariant Sets	3
Globalizing with Index Pairs	5
Symbolic Dynamics from Globalization	10
Discretization	14
Cubes, Representability and Enclosures	14
Invariant Parts by Depth-First Search	16
Computing a Representable Isolating Neighborhood Contained in a Specified Set	18
One Dimensional Cohomology Computation	20
Retraction to a Graph	22
Generating Paths	23
Images of the Generating Paths	24
Pressing the Image Paths into G	25
Computing the Matrix	26
Retractions induced by Decomposition of the Isolating Neighborhood into Connected Components	27
Examples	28
Hénon Map	28
Area Preserving Hénon Map	31

An Application to Time Series Analysis	35
Experimental Assumptions and Notation	35
Implementation	39
Modeling of the System	40
Symbolic Dynamics from the Model	43
Analysis of Magnetoelastic Ribbon Experiment	47
Modulus of Continuity and envelopes	50

Summary

The Conley index theory was developed by Conley and his students (for an overview, see [4]) in late 1960s and early 1970. At that time, it applied to continuous-time dynamical systems and was meant to be a robust tool for studying isolated invariant sets and their gradient-like structure. The problem of extending the theory for discrete dynamical systems, posed already by Conley in [4] together with a suggestion that such an extension may provide a way of relating the dynamics of continuous-time systems to their discretizations, was successfully solved by J.W.Robbin and D.Salamon in [20] and independently by M.Mrozek in [18]. This extension and later observations that it can be further extended to special multivalued maps [10] led to applications of the ideas of Conley index theory to computer assisted proofs, [13], [14], [17], [28]. Later on, similar ideas proved to be useful in time series analysis [15], [16]. This work is meant to be a gentle introduction to the topic. We review the basics of the Conley index theory, without stepping into arduous algebraic details of its formal definition and proofs of its properties which are not essential if the main goal is applying these ideas to computer assisted proofs or time series analysis. Then, a method of reducing the problem to a combinatorial one is described, together with some details on how to obtain representable index pairs and compute homology in 2D. Finally, we discuss an application of the approach to time series analysis, where an index pair computation can be used to obtain results about what variety of time series data one may expect to collect from a given experiment. For more general statements of theorems and more extensive discussion of the topic the reader is advised to consult the references.

Chapter 1

Symbolic Description of Dynamics via Index Pairs

One of the main goals of the theory of dynamical systems is to describe the structure of invariant sets. A popular way of modeling the dynamics is via symbolic dynamics: the invariant set is parameterized by a set of infinite sequences of symbols over some alphabet in such a way that its dynamics is equivalent to the dynamics of the shift map on that set of symbol sequences. Techniques based on the Conley index theory allow to obtain a slightly weakened variant of such a description as a result of the following two-stage process. In the first stage the problem is globalized. One substitutes the original dynamical system with a different one, defined by a self-map of a pointed compact topological space. The distinguished point is a local attractor. The dynamics on a neighborhood of the invariant part of the complement of the distinguished point is the same as on the neighborhood of the invariant set in the original system. An example of such a globalization for a hyperbolic fixed point on the plane this is shown in Figure 1. A small square containing the fixed point r whose edges are transversal to the stable and unstable manifolds of r is cut out of the phase space. Then, two triangles are glued to its edges intersected by the unstable manifold of r . Vertices of the two triangles are made meet at a point a which will be the dual attractor of r in the new system. From Figure 1, it should be apparent that the dynamics can be extended from the square to the entire new phase space in such a way that the dynamics around r is preserved and the attractor-repeller structure of the global invariant set is as described above. The next stage is essentially analysis of the topological structure of the new dynamical system. For our

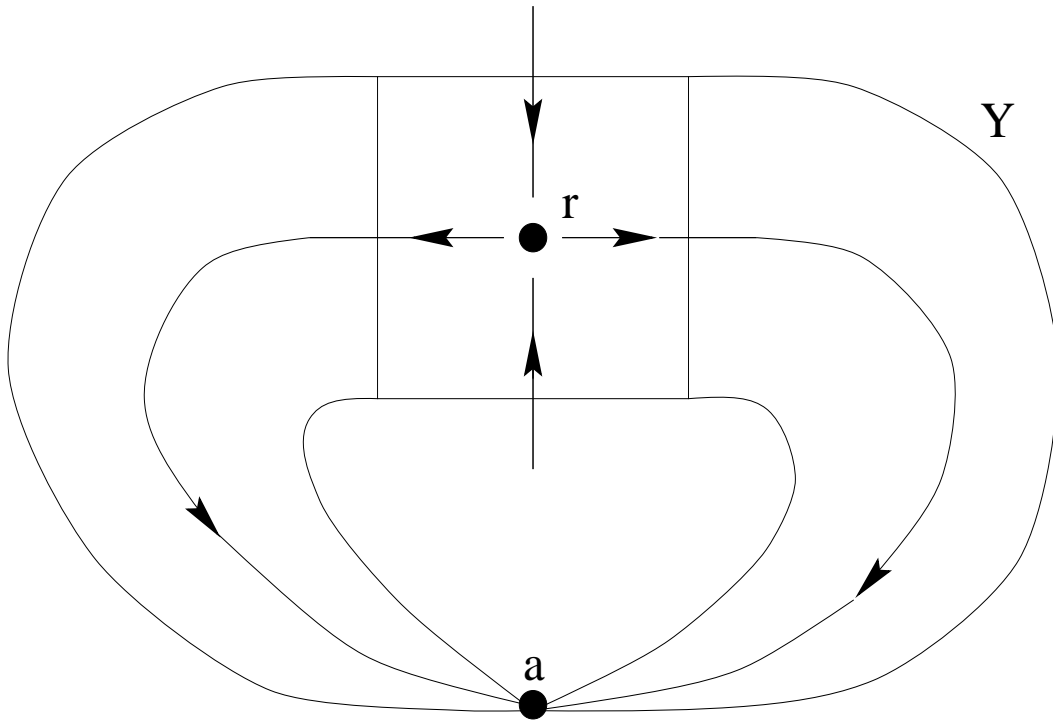


Figure 1: Globalization for a hyperbolic fixed point

hyperbolic fixed point one may compute the Lefschetz Number of the map induced by the new system on the pointed space (Y, a) . Since it is -1 , the Lefschetz Fixed Point Theorem implies the existence of a fixed point different from a in the new dynamical system. Any such fixed point belongs to the dual repeller of a , which is an exact copy of the invariant set we wanted to describe. Thus, we have shown that that invariant set contains a fixed point. Of course, this is not surprising since the invariant set is a hyperbolic fixed point. However, as we shall see later, our approach applies in much more general settings and can be used for detecting far more complicated dynamical features than fixed points. Moreover, it is robust under perturbation: the construction in Figure 1 goes through also for dynamical systems close to the original one in the C^0 sense. This is the main reason for the strength of our approach. First of all, it implies that it is not necessary to know the dynamical

system exactly in order to describe its dynamics. Secondly, it means that when this type of analysis is applied to models of physical processes, the physically insignificant properties of the dynamics are automatically filtered out. By ‘physically insignificant properties’ we mean properties which are either too fragile to be noticed and measured in an experimental system in a repeatable way or are too small in magnitude to be observed.

In the rest of this chapter we introduce the concept of an isolating neighborhood and isolated invariant set and define index pairs which provide a general way of globalizing the dynamics of an isolated invariant set. Then, we describe a way of obtaining a symbolic description for the globalized system (and hence for the original one since both are equivalent).

1.1 Isolated Invariant Sets

Although most dynamical systems which are interesting for general mathematical audience are single-valued, multivalued maps have proven to be an extremely powerful tool in the Conley index theory (see [9], [26], [31], [13], [10] for examples). Because of this, we shall give the basic definitions in the multivalued setting and make use of their generality later.

Throughout this section, F stands for a multivalued map of a locally compact metric space X into itself. We assume that F is upper semicontinuous, i.e. that for each open set $U \subset X$ the set of all points whose value under F is contained in U is open. We also assume that F maps each point into a closed set. A single valued map $f : X \rightarrow X$ can be treated as a special case of a multivalued map, sending a point x into the one-point set consisting of $f(x)$. Notice that this map is upper semicontinuous iff f is continuous.

Definition 1.1 A trajectory of F through x is a double-sided sequence $(x_i)_{-\infty}^{\infty}$ such that, for each $i \in \mathbf{Z}$, $x_{i+1} \in F(x_i)$ and $x = x_0$. A sequence with the above property indexed by \mathbf{Z}^- (\mathbf{Z}^+) will be called a backward (forward) trajectory.

Definition 1.2 The invariant part of a set $N \subset X$ under F , denoted by $\text{Inv}_F N$ is defined as the union of all trajectories of F contained in N .

Theorem 1.1 If N is compact then $\text{Inv}_F N$ is compact.

Proof. Define the double-sided sequence of sets $(N_i)_{-\infty}^{\infty}$ recursively by setting $N_0 = N$ and

$$N_i = \begin{cases} N \cap F(N_{i-1}) & \text{if } i > 0 \\ N \cap F^{-1}(N_{i+1}) & \text{if } i < 0, \end{cases}$$

where by $F^{-1}(A)$ for a set $A \subset X$ we mean the set of all points of X whose images intersect A . By upper semicontinuity of F , all N_i are compact. Since the invariant part of N is the intersection of N_i over $i \in \mathbf{Z}$, it is a compact set. \square

The following definition introduces the main object of interest in the Conley index theory: isolated invariant set. Although our definition is modeled after that in [10], it is not exactly the same: it does not involve the maximum diameter of an image of a point in N under F .

Definition 1.3 A compact set N is called an isolating neighborhood if and only if its invariant part is contained in its interior. A set S is called an invariant set iff its invariant part equals S . An invariant set which is an invariant part of some isolating neighborhood will be called an isolated invariant set.

We finish this section with a simple theorem which will be useful later on.

Theorem 1.2 Assume that F and G are multivalued maps of X into itself and that each point $x \in D \subset X$ has a neighborhood U such that $F(x) \subset \bigcap_{y \in U} G(y)$ and

$F(x) \subset \text{int } G(x)$. Any isolating neighborhood $N \subset D$ for G is also an isolating neighborhood for F and $\text{Inv}_F N \subset \text{int } \text{Inv}_G N$.

Proof. Take a trajectory (x_n) of F contained in N . Let $U \subset N$ be an open neighborhood of x_0 such that $F(x_0) \subset G(x)$ for all $x \in U$. Any double-sided sequence obtained from (x_n) by substituting x_0 with a point $y \in U \cap \text{int } G(x_{-1})$ is a trajectory of G . Therefore, $U \cap \text{int } G(x_{-1})$ is a neighborhood of x_0 in N contained in $\text{Inv}_G N$.
□

1.2 Globalizing with Index Pairs

This section describes a general way of globalizing the dynamics of an invariant set. We start with the definition of an index pair which plays a crucial role in this process. Like some of the other definitions given earlier, it differs slightly from those in [9], [10], [18], [25], [26] or [27]. However, in the single-valued case, it is a special case of the one in [20].

Definition 1.4 An index pair for a multivalued map $F : X \rightarrow X$ is a pair of compact sets (Q_1, Q_0) such that:

1. $F(Q_0 \cap \text{cl}(Q_1 \setminus Q_0)) \cap Q_1 \subset Q_0$
2. $F(Q_1 \setminus Q_0) \subset Q_1$
3. $\text{Inv}_F \text{cl}(Q_1 \setminus Q_0) \subset \text{int}(Q_1 \setminus Q_0)$

The following proposition is an immediate consequence of the above definition.

Proposition 1.1 Assume that F and G are multivalued maps such that $F(x) \subset G(x)$ for each $x \in X$. Any index pair for G is an index pair for F .

The next lemma will be used later on to construct index pairs.

Lemma 1.1 *Let $f : X \rightarrow X$ be a single-valued continuous map and F a multivalued upper semicontinuous map such that, for each $x \in D \subset X$, $F(x)$ is a closed neighborhood of $f(x)$ and there exists a neighborhood U of x such that $f(x) \in \bigcap_{y \in U} F(y)$. Let $N \subset D$ be an isolating neighborhood for F . Then:*

1. $N' := \text{Inv}_F N$ is an isolating neighborhood for f
2. For any compact set M such that $f(N') \subset M \subset F(N')$, the pair $(M \cup N', \text{cl}(M \setminus N'))$ is an index pair for f .
3. $(F(N'), \text{cl}(F(N') \setminus N'))$ is an index pair for f .

Proof. 1. By Theorem 1.2,

$$\text{Inv}_f N' \subset \text{Inv}_f N \subset \text{int } \text{Inv}_F N = \text{int } N'.$$

Hence N' is an isolating neighborhood for f .

2. Let $Q_1 = M \cup N'$ and $Q_0 = \text{cl}(M \setminus N')$. We have to show that (Q_1, Q_0) is an index pair for f . Clearly, $f(Q_1 \setminus Q_0) \subset f(N') \subset M \subset Q_1$. By the previous part,

$$\text{Inv}_f \text{cl}((M \cup N') \setminus (M \setminus N')) \subset \text{Inv}_f N' \subset \text{int } N' \subset \text{int}((M \cup N') \setminus \text{cl}(M \setminus N')).$$

It remains to show that $f(Q_0 \cap \text{cl}(Q_1 \setminus Q_0)) \cap Q_1 \subset Q_0$. Assume the contrary and take $x \in Q_0 \cap \text{cl}(Q_1 \setminus Q_0)$ such that $f(x) \in Q_1 \setminus Q_0$. Since $f(x) \in N'$, there is a forward trajectory of F through $f(x)$ contained in N . There is a neighborhood $U \subset N$ of x such that $f(x) \in F(y)$ for each $y \in U$. Thus, there is a forward trajectory of F in N through any point of U . U intersects $M \setminus N'$ and any point in the intersection has a backward trajectory (of F) through it contained in N , since $M \subset F(N')$. By merging the two half-trajectories one can obtain a trajectory of F in N through such

a point. Hence any such point is in N' , which is a contradiction.

3. Follows from part 2 applied for $M = F(N')$. \square

We shall call an index pair *stable* if it is an index pair for any map g close enough to f in the compact-open topology sense. The simplicity of the proof of the theorem below demonstrates the power of the multivalued approach to the Conley index. For a slightly different proof of the same theorem, the reader is referred to [9].

Theorem 1.3 *Let $f : X \rightarrow X$ be a single-valued map of a locally compact space and N be an isolating neighborhood for f . There exists a stable index pair $Q = (Q_1, Q_0)$ with $Q_1 \subset N$ and $\text{Inv}_f \text{cl}(Q_1 \setminus Q_0) = \text{Inv}_f N$.*

Proof. For any positive real number ϵ , let the multivalued map F_ϵ be defined by $F_\epsilon(x) := \bar{B}_\epsilon(f(x))$. For ϵ small enough, $N_\epsilon = \text{Inv}_{F_\epsilon} N \subset \text{int } N$ and $F_\epsilon(N_\epsilon) \subset N$. By Lemma 1.1,

$$Q = (F_\epsilon(N_\epsilon), \text{cl}(F_\epsilon(N_\epsilon) \setminus N_\epsilon))$$

is an index pair for f . Since the assumptions of the Lemma are satisfied for any map sufficiently close to f on N , Q is in fact a stable index pair. \square

An important consequence of the above theorem is that, in principle, the globalization method described here can be applied to any isolated invariant set. Stability of the index pair is also important since it means that it is an index pair also for small perturbations of the original dynamical system. With some additional mild assumptions (which seem to never fail in practice), this property ensures that the symbolic description of the dynamics obtained using our method is robust under small perturbations of the dynamics. The reader is advised to consult the references [4], [9], [10], [12], [13], [14], [18], [20], [22], [25] or [27] to find out more about the robustness property also known as the *homotopy continuation property* in the Conley index theory.

In the sequel, for a pair of compact subsets (Q_1, Q_0) of X by Q_1/Q_0 we shall mean the space resulting from Q_1 when the points of Q_0 are identified to a single distinguished point, denoted by $[Q_0]$.

Definition 1.5 (taken from [20]) *A pair (Q_1, Q_0) is called a weak index pair for a single-valued map $f : X \rightarrow X$ if and only if $\text{Inv}_f \text{cl}(Q_1 \setminus Q_0) \subset \text{int}(Q_1 \setminus Q_0)$ and the map $f_Q : Q_1/Q_0 \rightarrow Q_1/Q_0$ (called the index map) given by*

$$f_Q([x]) = \begin{cases} [f(x)] & \text{if } x, f(x) \in Q_1 \setminus Q_0 \\ [Q_0] & \text{otherwise} \end{cases}$$

is continuous.

The following simple theorem shows that any index pair is a weak index pair. In particular, it implies that weak index pairs exist for any isolated invariant set.

Theorem 1.4 *Any index pair for a single valued map $f : X \rightarrow X$ is a weak index pair.*

Proof. It is enough to show that the map $\tilde{f}_Q : Q_1 \rightarrow Q_1/Q_0$ given by $\tilde{f}_Q(x) = \tilde{f}_Q([x])$ is continuous at any point $x \in Q_1$. Consider four cases:

1. $x, f(x) \in Q_1 \setminus Q_0$. Then, for all y in some neighborhood of x in Q_1 , $y, f(y) \in Q_1 \setminus Q_0$. Therefore, $\tilde{f}_Q(y) = [f(y)]$ which proves the continuity of \tilde{f}_Q at x .
2. $f(x) \in Q_0$. Let U be a neighborhood of $[Q_0]$ in Q_1/Q_0 . Take a neighborhood V of Q_0 such that $V \cap Q_1 \subset \pi^{-1}(U)$, where $\pi : Q_1 \rightarrow Q_1/Q_0$ is the projection map. For all y in some neighborhood of x , f maps y into a point of V and hence \tilde{f}_Q maps $[y]$ into U . Thus, \tilde{f}_Q is continuous at x .
3. $f(x) \notin Q_1$ or $x \notin Q_1$. Then, $f(y) \notin Q_1$ or $y \notin Q_1$ for all y in some neighborhood of x . Hence \tilde{f}_Q is constant on a neighborhood of x and therefore continuous at x .

4. $x \in Q_0$ and $f(x) \in Q_1 \setminus Q_0$. By Definition 1.4 (1.), $x \notin \text{cl}(Q_1 \setminus Q_0)$, and therefore it has a neighborhood disjoint from $Q_1 \setminus Q_0$. Thus \tilde{f}_Q is locally constant and therefore continuous at x .

□

Weak index pairs provide a general way of globalizing the problem of describing the dynamics of an invariant set and therefore enable the use of the algebraic topological tools for this task. The following proposition makes this precise.

Proposition 1.2 *Let $Q = (Q_1, Q_0)$ be a weak index pair for f and $S = \text{Inv}_f \text{cl}(Q_1 \setminus Q_0)$. The map f_Q has the following properties:*

1. *The dynamics of f_Q on $\text{Inv}_{f_Q}(Q_1/Q_0 \setminus [Q_0])$ is the same as the dynamics of f on S .*
2. *The distinguished point $[Q_0]$ has a neighborhood U in Q_1/Q_0 which is mapped into $[Q_0]$ by some iterate of f_Q*

Proof. 1. The projection map from Q_1 to Q_1/Q_0 defines the equivalence

2. Assume that no such neighborhood exists. Let $(U_n)_{n=0}^\infty$ be a decreasing sequence of compact neighborhoods of $[Q_0]$ such that $U_0 \cap \text{Inv}_{f_Q}(Q_1/Q_0 \setminus [Q_0]) = \emptyset$ and $f_Q^i(U_n) \subset U_0$ for $i = 0, 1, \dots, 2n$, $n \in \mathbf{N}$. For each $n \in \mathbf{N}$ there exists a point $[x_n] \in U_n$ such that $f_Q^i([x_n]) \neq [Q_0]$ for $0 \leq i \leq 2n$. Then, $f^i(x_n) \in M = \{x \in Q_1 \setminus Q_0 : [x] \in U_0\}$ and therefore all cluster points of $f^n(x_n)$ are in $\text{cl } M$. Pick such a cluster point x_* . The diagonal method allows to construct a trajectory of f through x_* contained in $\text{cl } M$. This contradicts $S \cap M = \emptyset$. □

1.3 Symbolic Dynamics from Globalization

Let (Y, y_0) be a pointed compact metric space and $g : (Y, y_0) \rightarrow (Y, y_0)$ a continuous map. Assume that $\{A_i\}_{i=1}^k$ is a family of compact subsets of Y whose union is Y and such that each two intersect at y_0 . We can define continuous maps $r_i : (Y, y_0) \rightarrow (Y, y_0)$ by the following formula:

$$r_i(y) = \begin{cases} y & \text{if } y \in A_i \\ y_0 & \text{otherwise.} \end{cases}$$

Let $g_i = g \circ r_i$. The rest of this section demonstrates how these maps can be used to describe the invariant part of $Y \setminus y_0$ with respect to g in terms of symbolic dynamics. We start with the following simple proposition, whose proof is left to the reader.

Proposition 1.3 *If $y \in Y$ satisfies $g_{i_n} \circ g_{i_{n-1}} \circ \dots \circ g_{i_0}(y) \neq y_0$ then $g^j(y) \in A_{i_j} \setminus y_0$ for $j = 0, 1, \dots, n$.*

Definition 1.6 *We shall say that the point y_0 is a strong sink for g if and only if there exists a neighborhood U of y_0 and a natural number n such that $g^n(U) = \{y_0\}$.*

Maps as in Definition 1.6 arise naturally as index maps (cf Proposition 1.2; note that Q_1/Q_0 is metrizable by the Urysohn's Metrization Theorem; see [23]).

Corollary 1.1 *Assume that y_0 is a strong sink for g . If the sequence $(i_j)_{j=0}^\infty$ such that $i_j \in \{1, 2, \dots, k\}$ has the property that the composition $g_{i_j} \circ g_{i_{j-1}} \circ \dots \circ g_{i_0}$ is not the constant map into y_0 for each $j \in \mathbf{Z}^+$ then there exists $y \in Y$ such that $y_0 \neq g^j(y) \in A_{i_j}$ for each $j \in \mathbf{Z}^+$.*

Proof. By Proposition 1.3, for each $j \in \mathbf{Z}^+$ there exists z_j ($j \in \mathbf{Z}^+$) such that $g_{i_j} \circ g_{i_{j-1}} \circ \dots \circ g_{i_0}(z_j) \neq y_0$. Define

$$z_{j,l} = g_{i_l} \circ g_{i_{l-1}} \circ \dots \circ g_{i_0}(z_j).$$

Thus, $z_{j,j} \neq y_0$ for all j . Notice that

$$z_{j,j} = g_{i_j} \circ g_{i_{j-1}} \circ \dots \circ g_{i_{m+1}}(z_{j,m})$$

for $j \geq m$. Since

$$g_{i_j} \circ g_{i_{j-1}} \circ \dots \circ g_{i_{m+1}}(U) = \{y_0\}$$

provided $j \geq m + n$, it follows that $z_{j,m} \notin U$ for such j and m . Let y be a cluster point of (z_j) . Since for any $l \in \mathbf{Z}^+$ $g_{i_l} \circ g_{i_{l-1}} \circ \dots \circ g_{i_0}(y)$ is a cluster point of $(z_{j,l})_{j=0}^\infty$,

$$g_{i_m} \circ g_{i_{m-1}} \circ \dots \circ g_{i_0}(y) \neq y_0$$

for all m . By Proposition 1.3, the point y has the required properties. \square

Recall that, for Y being an ANR, the Lefschetz number of a map $h : (Y, y_0) \rightarrow (Y, y_0)$, denoted by $\Lambda(h)$, is defined as

$$\Lambda(h) = \sum_{i=0}^{\infty} (-1)^i \operatorname{tr} H_i(h) = \sum_{i=0}^{\infty} (-1)^i \operatorname{tr} H^i(h),$$

where by H_i and H^i we denote the i -dimensional homology and cohomology functors with coefficients in \mathbf{Q} . In order to obtain algebraic criteria for existence of periodic points we are going to use some of the properties of the fixed point index. For more details on the Lefschetz number and the necessary information about the fixed point index the reader is referred to [2].

Corollary 1.2 *Assume that Y is an ANR and the Lefschetz number of the composition $g_{i_{p-1}} \circ g_{i_{p-2}} \circ \dots \circ g_{i_0} : (Y, y_0) \rightarrow (Y, y_0)$ is nonzero. Then, g has a p -periodic point $y \neq y_0$ such that $g^j(y) \in A_{i_j}$ for each $j = 0, 1, \dots, p-1$.*

Proof. Since y_0 is a strong sink for the composition map, it is an isolated fixed point and its index is 1. The fixed point index of the set of all fixed points of the composition map is equal to the Lefschetz number plus 1. If that Lefschetz number

is nonzero, the index is not equal to the index of y_0 and therefore the composition map has a fixed point different from y_0 . Such a point y is a p -periodic point of g and

$$y_0 \neq g_{i_{p-1}} \circ g_{i_{p-2}} \circ \dots \circ g_{i_0}(y) = y.$$

By Proposition 1.3, $g^j(y) \in A_{i_j}$ for $j \in \{0, 1, \dots, p-1\}$. \square

We finish this section with a restatement of the above theorems in the language of symbolic dynamics. Let $\Pi = \prod_{i=0}^{\infty} \{1, 2, \dots, k\}$. By S^+ we shall denote the positively invariant part of $Y \setminus y_0$, i.e. the union of all forward trajectories of g contained in $Y \setminus y_0$. S will stand for the invariant part of $Y \setminus y_0$. It is not hard to see that S^+ is a compact set and $S = \bigcap_{t=0}^{\infty} g^t(S^+)$. By σ we shall denote the shift map on Π . Define the continuous map $q : S^+ \rightarrow \Pi$ by

$$q(y) = (i_j)_{j=0}^{\infty} \iff g^j(y) \in A_{i_j} \text{ for all } j \in \mathbf{Z}^+.$$

Clearly, $q \circ f|_{S^+} = \sigma \circ q$. Below we provide lower bounds for the complexity of the dynamics of S .

Definition 1.7 *For a functor F defined on the category of pointed topological spaces, let*

$$\Pi_F((Y, y_0), g, \{A_i\}_{i=1}^k) := \bigcap_{t=0}^{\infty} \sigma^t \left(\left\{ (i_j)_{j=0}^{\infty} : F(g_{i_j} \circ g_{i_{j-1}} \circ \dots \circ g_{i_0}) \neq F(c_{y_0}) \right. \right. \\ \left. \left. \text{for all } j \in \mathbf{Z}^+ \right\} \right),$$

where c_{y_0} is the constant map into y_0 .

Assuming that Y is an ANR and $n \in \mathbf{N}$ we define

$$\text{Per}_n((Y, y_0), g, \{A_i\}_{i=1}^k) := \left\{ (i_j)_{j=0}^{\infty} : (i_j) \text{ is } n\text{-periodic and} \right. \\ \left. \Lambda(g_{i_{n-1}} \circ g_{i_{n-2}} \circ \dots \circ g_{i_0}) \neq 0 \right\}.$$

The following theorem is a consequence of Corollary 1.1 and 1.2.

Theorem 1.5 1. $\Pi_F((Y, y_0), g, \{A_i\}_{i=1}^k) \subset q(S)$ for any functor F

2. $\text{Per}_n((Y, y_0), g, \{A_i\}_{i=1}^k)$ is contained in the image of the set of n -periodic points of f in S under q . Note that if a sequence $\iota \in \text{Per}_n((Y, y_0), g, \{A_i\}_{i=1}^k)$ is of least period n then any n -periodic point mapped into ι by q has to be of least period n .

Proof. 1. By Corollary 1.1,

$$q(S^+) \supset \Pi_0 := \left\{ (i_j)_{j=0}^\infty : F(g_{i_j} \circ g_{i_{j-1}} \circ \dots \circ g_{i_0}) \neq F(c_{y_0}) \text{ for all } j \in \mathbf{Z}^+ \right\}.$$

Thus, $q(g^t(S^+)) \supset \sigma^t(\Pi_0)$ for each $t \in \mathbf{Z}^+$. By compactness of S^+ ,

$$\Pi_F((Y, y_0), g, \{A_i\}_{i=1}^k) = \bigcap_{t=0}^\infty \sigma^t(\Pi_0) \subset \bigcap_{t=0}^\infty q(g^t(S^+)) \subset q\left(\bigcap_{t=0}^\infty g^t(S^+)\right) = q(S).$$

2. follows immediately from Corollary 1.2. The second statement follows from the definition of q . \square

Chapter 2

Discretization

The approach presented in the previous section can be used to reduce the problem of describing the dynamics in terms of symbols to a purely combinatorial computation. This section explains the details of how such a reduction can be done. We shall start with a few definitions which allow one to convert the problem on the continuous level to an analogous one on the discrete level. Then, we describe an algorithm for constructing representable isolating neighborhoods and index pairs. Finally, we briefly discuss one-dimensional homology computation and give a few examples where our approach can be used to obtain interesting information about the dynamics of an isolated invariant set. Most of the results presented in this section can be found in [28].

2.1 Cubes, Representability and Enclosures

Subsets of \mathbf{R}^n are often represented on a computer as unions of grid cubes. We shall follow this approach here since it is very simple and appears sufficient for our purposes.

Fix positive real numbers $\epsilon_1, \epsilon_2, \dots, \epsilon_n$ and let ϵ be the smallest of them. By a *grid cube* we shall mean a subset of \mathbf{R}^n of the form

$$[k_1\epsilon_1, (k_1 + 1)\epsilon_1] \times [k_2\epsilon_2, (k_2 + 1)\epsilon_2] \times [k_n\epsilon_n, (k_n + 1)\epsilon_n],$$

where k_1, k_2, \dots, k_n are integers. By Ω we shall denote the set of all grid cubes. For a subset \mathcal{A} of Ω by $|\mathcal{A}|$ we denote the subset of Ω represented by \mathcal{A} , i.e. the union of all grid cubes in \mathcal{A} . By $o(\mathcal{A})$ we denote the set of all grid cubes intersecting $|\mathcal{A}|$. In other words, $o(\mathcal{A})$ is the representation of the smallest representable neighborhood of $|\mathcal{A}|$.

Let \mathcal{F} be a multivalued map of Ω into itself such that $\mathcal{F}(K)$ is finite for each $K \in \Omega$. In what follows, we shall think of \mathcal{F} as a dynamical system, in particular, we shall apply to it some of the definitions from the previous chapter (like that of the invariant part).

Let $f : \mathbf{R}^n \rightarrow \mathbf{R}^n$ be a single-valued continuous map. The following definition introduces a way to finitely represent f .

Definition 2.1 *A multivalued map $\mathcal{F} : \Omega \rightarrow \Omega$ is an enclosure of f if and only if $f(K) \subset \text{int}|\mathcal{F}(K)|$ for any $K \in \Omega$.*

The following theorem shows that such a finite representation of the map f can be used to obtain isolating neighborhoods and index pairs.

Theorem 2.1 *Let \mathcal{N} be a finite subset of Ω such that $\mathcal{N} = \text{Inv}_{\mathcal{F}o}(\mathcal{N})$ where \mathcal{F} is an enclosure of f . Then:*

1. $|\mathcal{N}|$ is an isolating neighborhood for f
2. $(|\mathcal{F}(\mathcal{N})|, |\mathcal{F}(\mathcal{N}) \setminus \mathcal{N}|)$ is an index pair for f .

Proof.

1. Assume the contrary. Let $(x_j)_{j=-\infty}^{\infty}$ be a trajectory of f with $x_0 \in \text{bd}|\mathcal{N}|$. For each j , let K_j be a grid cube containing x_j , with K_0 chosen so that it is not in \mathcal{N} . Then, (K_j) is a trajectory of \mathcal{F} contained in $o(\mathcal{N})$. Therefore, $K_0 \in \text{Inv}_{\mathcal{F}o}(\mathcal{N}) = \mathcal{N}$. This is a contradiction.

2. Since $\text{cl}(|\mathcal{F}(\mathcal{N})| \setminus |\mathcal{F}(\mathcal{N}) \setminus \mathcal{N}|) = |\mathcal{N}|$, we have just proven that the third condition in Definition 1.4 is satisfied. Also,

$$f(|\mathcal{F}(\mathcal{N})| \setminus |\mathcal{F}(\mathcal{N}) \setminus \mathcal{N}|) \subset f(|\mathcal{N}|) \subset |\mathcal{F}(\mathcal{N})|,$$

which proves the second condition. It remains to prove that

$$f(|\mathcal{F}(\mathcal{N}) \setminus \mathcal{N}| \cap |\mathcal{N}|) \cap |\mathcal{F}(\mathcal{N})| \subset |\mathcal{F}(\mathcal{N}) \setminus \mathcal{N}|.$$

Assume the contrary. There is an $x \in |\mathcal{F}(\mathcal{N}) \setminus \mathcal{N}| \cap |\mathcal{N}|$ such that $f(x) \in |\mathcal{F}(\mathcal{N})| \setminus |\mathcal{F}(\mathcal{N}) \setminus \mathcal{N}|$. Let L be a grid cube in $\mathcal{F}(\mathcal{N}) \setminus \mathcal{N}$ containing x . Take $K \in \mathcal{N}$ such that $L \in \mathcal{F}(K)$. Since $f(x) \in |\mathcal{N}|$, there is an $M \in \mathcal{N}$ such that $f(x) \in M$. Such an M is also in $\mathcal{F}(L)$. Since K and M are in \mathcal{N} , they have a backward and forward trajectories (respectively) contained in \mathcal{N} , which we shall denote by $(K_j)_{j=-\infty}^0$ and $(M_j)_{j=0}^{\infty}$. The double-sided sequence (L_j) defined by

$$L_j = \begin{cases} L & \text{if } j = 0 \\ K_{j+1} & \text{if } j < 0 \\ M_{j-1} & \text{if } j > 0. \end{cases}$$

is a trajectory of \mathcal{F} through L contained in $o(\mathcal{N})$. Thus, $L \in \text{Inv}_{\mathcal{F}o}(\mathcal{N}) = \mathcal{N}$. However, L was chosen from $\mathcal{F}(\mathcal{N}) \setminus \mathcal{N}$. This is a contradiction.

□

2.2 Invariant Parts by Depth-First Search

A multivalued map $\mathcal{F} : \Omega \rightarrow \Omega$ on a finite subset \mathcal{N} of Ω will be represented as a set of records, one per element of \mathcal{N} . Each record corresponding to $K \in \mathcal{N}$ will contain a list of elements of \mathcal{N} in the image of K under \mathcal{F} and a list of elements of \mathcal{N} in the inverse image of K .

```

var
   $\mathcal{I}, \mathcal{D}$  : subset of  $\Omega$ ;

function rec_inv_plus ( a: element of  $\Omega$  ) : boolean;
begin
  if  $a \in \mathcal{I}$  return TRUE;
  if  $a \in \mathcal{D}$  return FALSE;
   $\mathcal{I} := \mathcal{I} \cup \{a\}$ ;
  for each  $b \in \mathcal{F}(a) \cap \mathcal{N}$  do :
    if rec_inv_plus(b) then
      return TRUE;
   $\mathcal{I} := \mathcal{I} \setminus \{a\}$ ;
   $\mathcal{D} := \mathcal{D} \cup \{a\}$ ;
  return FALSE;
end;

function inv_plus (  $\mathcal{N}$ : subset of  $\Omega$  ) : subset of  $\Omega$ ;
begin
   $\mathcal{I} := \emptyset$ ;  $\mathcal{D} := \emptyset$ ;
  for each  $a \in \mathcal{N}$  do rec_inv_plus(a);
  return  $\mathcal{I}$ ;
end;

```

Figure 2: Pseudocode for the positively invariant part computation (function `inv_plus`)

The invariant part of \mathcal{N} with respect to \mathcal{F} is the intersection of its positively and negatively invariant parts. The negatively (positively) invariant part is the union of all backward (forward) trajectories of \mathcal{F} contained in \mathcal{N} .

The pseudocode of the procedure for computing the positively invariant part is given in Figure 2. If the sets \mathcal{I} and \mathcal{D} are stored as characteristic functions (i.e. by giving each of the elements of \mathcal{N} a flag saying if that element is in the set or not, so that insertion/deletion of an element takes a constant time) then the running time of the above procedure is linear.

Since forward trajectories correspond to backward trajectories via time reversal, the negatively invariant part can be computed in linear time in an analogous way.

The invariant part, being the intersection of the positively and negatively invariant parts, can be determined from the results in linear time.

The input data for the procedure in Figure 2 can be looked at as a directed graph whose vertices correspond to elements of \mathcal{N} and edges join an element of $K \in \mathcal{N}$ to an element of $\mathcal{F}(K)$. The positively invariant part computation is based on the following two principles:

1. all elements of \mathcal{N} on any path ending at an element of the positively invariant set are in the positively invariant set;
2. all elements of \mathcal{N} on a path starting at an element of \mathcal{N} and ending on an element which has been visited by that path before are in the positively invariant part.

The set \mathcal{I} in the procedure on Figure 2 consists of the elements which have already been decided to be in the positively invariant part, either by finding a ‘witness’ path (principle 2.) or by finding a path through it ending at a cube already known to be in the positively invariant part (principle 1.). The paths are searched exhaustively via depth-first search. Recursing is terminated when an element in the set \mathcal{D} is encountered. The set \mathcal{D} consists of all elements which have been decided not to belong to the positively invariant part. An element $K \in \mathcal{N}$ is added to \mathcal{D} whenever no path as described in 1. and 2. above starting at K is found.

2.3 Computing a Representable Isolating Neighborhood Contained in a Specified Set

Representable isolating neighborhoods for which a computation yielding interesting results can be performed at the prescribed level of detail tend to be complicated and hard to specify manually (see examples in the following sections). In this section

we describe an algorithm for constructing an isolating neighborhood contained in a given representable set. Let us start with a theorem providing the abstract background for the algorithm. Throughout this section, \mathcal{F} stands for an enclosure for a continuous single-valued function f .

Theorem 2.2 *Let \mathcal{B} be a finite subset of Ω . Put $\mathcal{B}_0 = \mathcal{B}$. Let \mathcal{B}_i and \mathcal{C}_i ($i = 1, 2, \dots, m$) be subsets of Ω satisfying the following conditions.*

$$\text{Inv}_{\mathcal{F}}(\mathcal{B}_{i-1}) = \mathcal{B}_i \cup \mathcal{C}_i, \quad (1)$$

$$o(\mathcal{B}_i) \cap \mathcal{C}_i = \emptyset, \quad (2)$$

$$o(\mathcal{B}_m) \subset \mathcal{B}. \quad (3)$$

Then $\mathcal{B}_m = \text{Inv}_{\mathcal{F}}(o(\mathcal{B}_m) \cup \mathcal{C}_m) \cap o(\mathcal{B}_m)$.

Proof. $\mathcal{U}_i = \mathcal{C}_1 \cup \mathcal{C}_2 \cup \dots \cup \mathcal{C}_i$, $i = 0, 1, \dots, m$. We prove inductively that $\text{Inv}_{\mathcal{F}}(\mathcal{B} \setminus \mathcal{U}_i) = \text{Inv}_{\mathcal{F}}(\mathcal{B}_i)$. It is obvious for $i = 0$. Supposing that this equality holds for some $i < m$ and using (1) and (2), we obtain

$$\begin{aligned} \text{Inv}_{\mathcal{F}}(\mathcal{B} \setminus \mathcal{U}_{i+1}) &= \text{Inv}_{\mathcal{F}}((\mathcal{B} \setminus \mathcal{U}_i) \setminus \mathcal{C}_{i+1}) \subset \text{Inv}_{\mathcal{F}}(\mathcal{B} \setminus \mathcal{U}_i) \setminus \mathcal{C}_{i+1} = \\ &= \text{Inv}_{\mathcal{F}}(\mathcal{B}_i) \setminus \mathcal{C}_{i+1} = \mathcal{B}_{i+1}. \end{aligned}$$

Hence $\text{Inv}_{\mathcal{F}}(\mathcal{B} \setminus \mathcal{U}_{i+1}) \subset \text{Inv}_{\mathcal{F}}(\mathcal{B}_{i+1})$. Since $\mathcal{B}_{i+1} \subset \mathcal{B} \setminus \mathcal{U}_{i+1}$, the converse inclusion holds and the proof is finished. By (2) and (3), $o(\mathcal{B}_m) \subset \mathcal{B} \setminus \mathcal{U}_m$. It follows that

$$\begin{aligned} \text{Inv}_{\mathcal{F}}(o(\mathcal{B}_m) \cup \mathcal{C}_m) \cap o(\mathcal{B}_m) &\subset \text{Inv}_{\mathcal{F}}((\mathcal{B} \setminus \mathcal{U}_m) \cup \mathcal{C}_m) \cap o(\mathcal{B}_m) \subset \\ &\subset \text{Inv}_{\mathcal{F}}(\mathcal{B} \setminus \mathcal{U}_{m-1}) \cap o(\mathcal{B}_m) = \text{Inv}_{\mathcal{F}}(\mathcal{B}_{m-1}) \cap o(\mathcal{B}_m) = \\ &= (\mathcal{B}_m \cup \mathcal{C}_m) \cap o(\mathcal{B}_m) = \mathcal{B}_m. \end{aligned}$$

To see that the reverse inclusion is true notice that $\mathcal{B}_m \subset o(\mathcal{B}_m)$ and

$$\mathcal{B}_m \subset \text{Inv}_{\mathcal{F}}(\mathcal{B}_{m-1}) = \text{Inv}_{\mathcal{F}}\text{Inv}_{\mathcal{F}}(\mathcal{B}_{m-1}) \subset \text{Inv}_{\mathcal{F}}(\mathcal{B}_m \cup \mathcal{C}_m) \subset \text{Inv}_{\mathcal{F}}(o(\mathcal{B}_m) \cup \mathcal{C}_m)$$

□

Theorems 2.1 and 2.2 imply the following corollary.

```

function index_pair (  $\mathcal{N}$  : subset of  $\Omega$  ) : pair of subsets of  $\Omega$ ;
var  $\mathcal{D}, \mathcal{A}$  : subset of  $\Omega$ ;
begin
   $\mathcal{D} := d(\mathcal{N});$            //  $d(\mathcal{N}) = o(\Omega \setminus \mathcal{N})$ 
   $\mathcal{A} := \text{Inv}_{\mathcal{F}}\mathcal{N};$ 
  while ( $\mathcal{D} \cap \mathcal{A} \neq \emptyset$ ) do:
    choose a  $K \in \mathcal{A}$ ;
     $\mathcal{A} := \mathcal{A} \setminus \text{conn\_comp}(K, \mathcal{A});$ 
     $\mathcal{A} := \text{Inv}_{\mathcal{F}}\mathcal{A};$ 
  return ( $\mathcal{F}(\mathcal{A}), \mathcal{F}(\mathcal{A}) \setminus \mathcal{A}$ );
end;

```

Figure 3: Computing index pairs

Corollary 2.1 *If the sets \mathcal{B}_i and \mathcal{C}_i are as in Theorem 2.2 and $\mathcal{C}_m = \emptyset$ then $\mathcal{B}_m = \text{Inv}_{\mathcal{F}o}(\mathcal{B}_m)$. Thus, if \mathcal{F} is an enclosure for a single-valued continuous map f then $\mathcal{N} = \mathcal{B}_m$ represents an isolating neighborhood for f and $(|\mathcal{F}(\mathcal{N})|, |\mathcal{F}(\mathcal{N}) \setminus \mathcal{N}|)$ is an index pair for f .*

An easy consequence of Corollary 2.1 is that the `index_pair` function on Figure 3, when called for a subset \mathcal{N} of Ω , returns the representation of an index pair for f , i.e. a pair $(\mathcal{Q}_1, \mathcal{Q}_0)$ of subsets of Ω such that $(|\mathcal{Q}_1|, |\mathcal{Q}_0|)$ is an index pair for f . The call `conn_comp(K, \mathcal{A})` returns the subset of Ω representing the connected component of \mathcal{A} containing K and can be implemented as a special case of an algorithm for computing a connected component in a graph [5]. Note that in the procedure `index_pair` the choice of K within the loop is arbitrary and by changing the criteria for making that choice one may obtain different index pairs.

2.4 One Dimensional Cohomology Computation

This section outlines the basic steps of the procedure for computing the endomorphism induced by the index map on the one-dimensional cohomology over the field

of rational numbers. The idea is based on the algorithm for computing fundamental groups of graphs and on the concept of a cell collapse (cf [7], [11]). Our presentation is, to some extent, influenced by the work on mesh compression [21] and [30]. In what follows, \mathcal{F} stands for an enclosure of a continuous map $f : \mathbf{R}^2 \rightarrow \mathbf{R}^2$ and $(\mathcal{Q}_1, \mathcal{Q}_0)$ is the representation of an index pair obtained using the algorithm described in the previous section. We shall further assume that $|\mathcal{F}(K)|$ is a rectangle for each $K \in \Omega$. The main steps of the algorithm are listed below.

1. Find a deformation retraction of $(|\mathcal{Q}_1|, |\mathcal{Q}_0|)$ to a graph G ;
2. Find paths generating $H_1(|\mathcal{Q}_1|/|\mathcal{Q}_0|)$ by finding a spanning tree of the graph G obtained in step 1 with all vertices in the exit set identified to one vertex and leading loops through edges in the complement of that tree (called *critical edges* later on);
3. Find homotopy classes of images of each of the generating paths under the index map by joining images of the consecutive vertices along each of the generating paths;
4. Project ('press') the image paths into G by applying the deformation retraction constructed in step 1.
5. Compute the coefficients of the matrix of the induced endomorphism by looking at how the paths in G which are homotopy equivalent to the images of generating paths pass through the critical edges.

The subsections below illustrate each of these steps. Since the methods used in this section are quite standard in combinatorial topology, we shall often skip the details and keep our discussion on a low level of abstraction. Since we will be dealing with

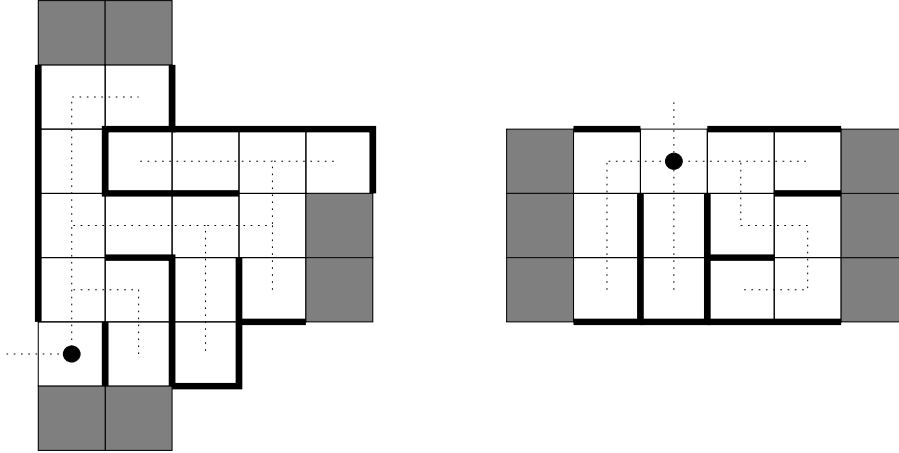


Figure 4: *Retraction to a graph.* The dotted lines correspond to edges of a spanning forest of the adjacency graph; the roots of the (in this example, two) trees are marked with black dots. Bold edges are edges of G , a graph being a retract of $(|\mathcal{Q}_1|, |\mathcal{Q}_0|)$. More precisely, $(|G| \cup |\mathcal{Q}_0|, |\mathcal{Q}_0|)$ is a strong deformation retract of that pair and the retraction can be obtained as a composition of square collapses [7] performed in an order given by a depth-first search traversal of each of the trees.

the two dimensional case, we shall call grid cubes *squares* (although in general they may be rectangles).

2.4.1 Retraction to a Graph

By the *adjacency graph* of the pair $(\mathcal{Q}_1, \mathcal{Q}_0)$ we mean the graph whose vertices correspond to squares in $\mathcal{Q}_1 \setminus \mathcal{Q}_0$ and edges join adjacent squares. A *boundary square* is a square in $\mathcal{Q}_1 \setminus \mathcal{Q}_0$ adjacent to one outside \mathcal{Q}_1 . For the rest of this chapter, we shall assume that each connected component of the adjacency graph contains a boundary square. This assumption is satisfied for all examples described further in this paper. Let us note that even if it is not, the computation does not necessarily have to fail - one can always delete components which do not contain a boundary square, obtaining another index pair for f , which definitely satisfies our assumption. We shall also assume that there are no connected components of $|\mathcal{Q}_1 \setminus \mathcal{Q}_0|$ which

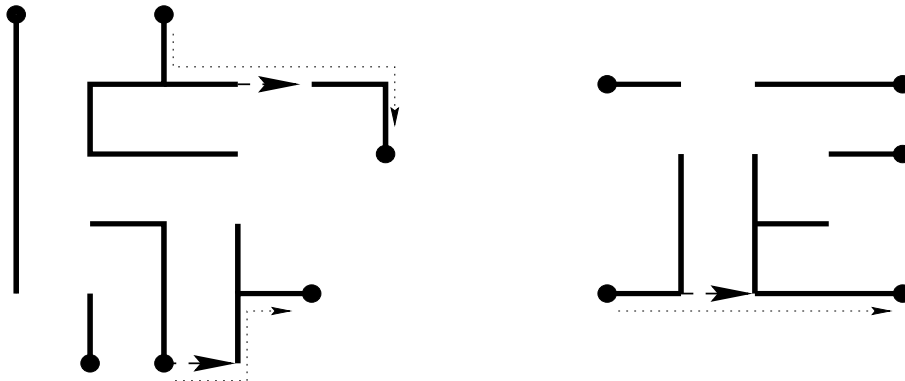


Figure 5: *Paths representing the generators of the one dimensional homology (shown as dotted lines).*

do not intersect $|\mathcal{Q}_0|$. It is not hard to see that those two assumptions are in fact equivalent to assuming that the cohomology of the pointed space $|\mathcal{Q}_1|/|\mathcal{Q}_0|$ is zero in dimensions 0 and 2.

In order to find a graph G being a retract of the pair $(|\mathcal{Q}_1|, |\mathcal{Q}_0|)$ we first find a spanning forest of the adjacency graph. Each tree of that forest is a spanning tree of the connected component containing it and will be thought of as rooted at one of its boundary squares. In Figure 4, the edges of the forest are drawn as dotted lines joining centers of the grid squares. For the root square, we draw another dotted line connecting its center to the center of an adjacent square in the complement of \mathcal{Q}_1 . G is defined as the set of those edges of the grid squares in \mathcal{Q}_1 which are *not* intersected by the dotted lines and are not edges of squares in \mathcal{Q}_0 .

2.4.2 Generating Paths

In order to find a set of paths forming a set of generators for $H^1(|\mathcal{Q}_1|, |\mathcal{Q}_0|)$, we first look for a spanning tree of the graph G' obtained from G by identifying its vertices lying in $|\mathcal{Q}_0|$ (black dots in Figure 5) to one vertex, denoted by q_0 . Efficient algorithms for computing a spanning tree are well known [5]. Edges of one possible

spanning tree are shown as bold solid lines in the Figure. Edges of the graph G' which do not belong to the spanning tree (later referred to as critical edges) are shown as large arrows. Paths generating the first homology group are shown as dotted lines. They are in one-to-one correspondence to the critical edges and can be obtained as follows. First, fix an orientation of each of critical edges arbitrarily (for example as indicated by arrows in the Figure). For each endpoint of such an edge there is a path connecting it to q_0 . In order to obtain a generating path corresponding to a critical edge, first follow a path from q_0 to the starting point of that edge. Then, move along the critical edge and follow a path joining its endpoint with q_0 .

2.4.3 Images of the Generating Paths

Assume that v_1, v_2, \dots, v_k are vertices along one of the generating paths. In order to compute the homotopy class of the image of that path under the index map we first pick an arbitrary vertex w_i of one of the squares in the intersection $\bigcap_{K \in \Omega: v_i \in K} \mathcal{F}(K)$ for each i . Then, we join each two consecutive vertices w_i, w_{i+1} with a path consisting of at most two straight line segments, first of which is horizontal and joins w_i with the point whose x -coordinate is the same as that of w_{i+1} . The second segment is vertical and joins the endpoint of the first one with w_{i+1} . This is illustrated in Figure 6. Notice that, since the basis paths start and end in $|\mathcal{Q}_0|$ and each square in \mathcal{Q}_0 is mapped by \mathcal{F} into a representation of a rectangle which does not intersect $|\mathcal{Q}_1| \setminus |\mathcal{Q}_0|$, the path described above starts and ends in $|\mathcal{Q}_0|$ and can leave or enter $|\mathcal{Q}_1| \setminus |\mathcal{Q}_0|$ only through $|\mathcal{Q}_0|$. Therefore, it defines a valid continuous loop in the quotient space $|\mathcal{Q}_1|/|\mathcal{Q}_0|$. Using the convexity of $|\mathcal{F}(K)|$ for $K \in \mathcal{Q}_1$ one can show that the path defined above and the image of the basis path under f are homotopic. More precisely, one shows that the convex combination of the two paths with varying coefficients defines a deformation of one path into the other.

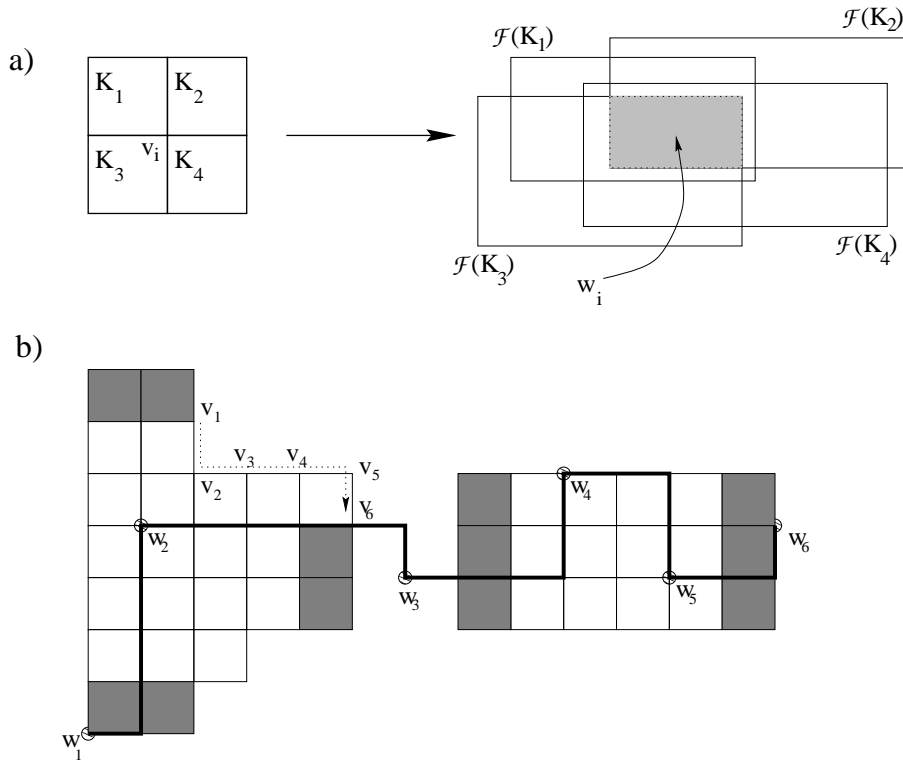
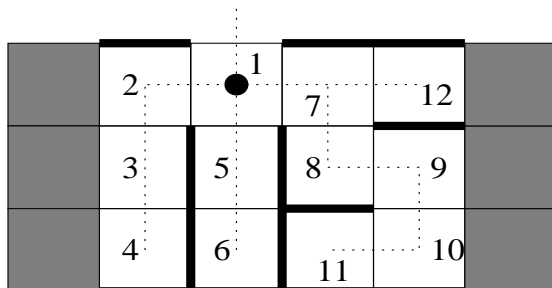


Figure 6: a) Selection of w_i , an arbitrary grid point in the intersection of the images of the four squares surrounding v_i ; b) Image (bold black line) of a basis path (dotted), constructed as described in Section 2.4.3

2.4.4 Pressing the Image Paths into G

The goal of this stage is to replace each of the image paths obtained above with a homotopy equivalent path which stays within G for the time it passes through $|\mathcal{Q}_1| \setminus |\mathcal{Q}_0|$. We do that as follows. First, do a depth-first search traversal of the spanning forest of the adjacency graph obtained in step 1., starting from the roots of each of its trees. Then, look at the grid squares in the traversal order (a possible traversal order for the component on the right of Figure 4 is shown in Figure 7a). For each square, consider its edge which is crossed by the tree edge along which the square was entered during the traversal. Substitute that edge in any of the image paths with the ‘detour’ path as shown in Figure 7b. After taking a detour we ‘simplify’ the path

a)



b)

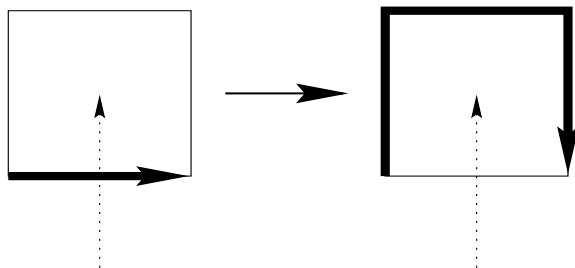


Figure 7: a) An example depth-first search traversal order; b) Detouring an edge of a grid square

by removing moves along an edge and then back in the next step. All stages of this process for the piece of the image path in Figure 6b within the component on the right are shown in Figure 8.

2.4.5 Computing the Matrix

It is now time to turn the results of the computations described above into the matrix B of the endomorphism induced by the index map on one dimensional cohomology. Let us number the critical edges with integers $1, 2, \dots, m$. B will be a $m \times m$ square matrix whose entry in i -th row and j -th column is given by the number of times the j -th critical edge appears along the path in G homotopic to the image of the

and that the critical edges between $(j_i + 1)$ -th and j_{i+1} -th are contained in C_i . Then, the matrices of the endomorphisms g_i^1 can be obtained from B by replacing all its entries which are above the $(j_i + 1)$ -th row or below the j_{i+1} -th row with zeroes. To make our notation concise, we shall indicate that by dividing the matrix B with horizontal lines into blocks, each of them corresponding to one of the A_i 's. For example, if there are two components of $|\mathcal{Q}_1| \setminus |\mathcal{Q}_0|$, the first one contains two critical edges, the second one - one critical edge and the f_Q map is homotopic to the identity then

$$B = \left[\begin{array}{ccc} 1 & 0 & 0 \\ 0 & 1 & 0 \\ \hline 0 & 0 & 1 \end{array} \right].$$

2.5 Examples

This section contains a brief description of two applications of the techniques described earlier in this chapter. We present results of the computation of the endomorphism induced on cohomology for certain index pairs of the Hénon map and the area preserving Hénon map. For a description of applications to the Lorenz Equations the reader is referred to [13], [14] and [17].

2.5.1 Hénon Map

The Hénon map, introduced in [8] (see also [19]), is a homeomorphism of the plane defined by

$$H(x, y) = (1 - ax^2 + y, bx).$$

a and b are constants, in the original paper being 1.4 and 0.3, respectively. The map H can be shown to have an attractor which exhibits complicated dynamics [19]. The

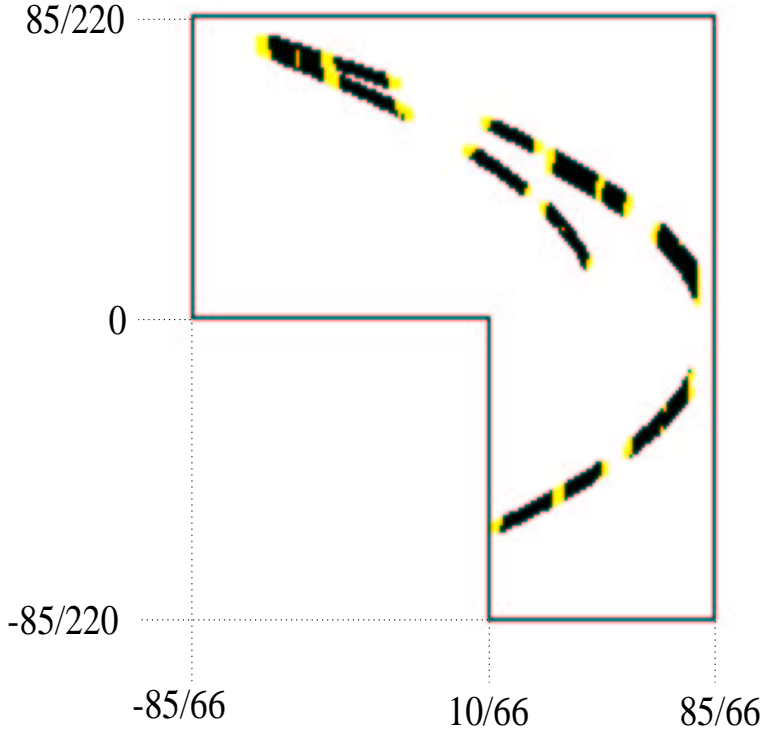


Figure 9: *An index pair for the Hénon map; the set Q_0 is shown gray and Q_1 consists of grid squares which are either black or gray.*

procedure outlined in the previous section can be used to find an index pair for H contained in the region whose boundary is shown as solid black line in Figure 9. The edges of grid cubes have lengths $\epsilon_1 = 1/66$ and $\epsilon_2 = 1/220$. Note that the ratio ϵ_2/ϵ_1 is equal to b - this is to make up for the scaling of x in the formula for the second coordinate. A representation of H as a multivalued map $\mathcal{H} : \Omega \rightarrow \Omega$ was computed using interval arithmetic. More precisely, to compute it for a grid square $K = [i_1\epsilon_1, (i_1 + 1)\epsilon_1] \times [i_2\epsilon_2, (i_2 + 1)\epsilon_2]$ we substitute x and y in the formula for H with intervals $[i_1\epsilon_1, (i_1 + 1)\epsilon_1]$ and $[i_2\epsilon_2, (i_2 + 1)\epsilon_2]$. As a result, we obtain a pair of intervals representing a rectangle R bounding $H(K)$. As $\mathcal{H}(K)$ we take the set of all grid rectangles intersecting R . The resulting index pair is shown in Figure 9. The cohomology computation procedure run for that index pair produces the following

matrix:

$$B = \begin{bmatrix} 0 & 0 & 0 & 0 & 0 & 0 & 0 & 0 & 0 & 0 & 0 & 0 & 0 & 0 & 0 & 1 & -1 \\ 0 & 0 & 0 & 0 & 0 & 0 & 0 & 0 & 0 & 0 & 0 & 0 & 1 & 0 & 0 & 0 & 0 \\ \hline 0 & 0 & 0 & 0 & 0 & 0 & 0 & 0 & 0 & 0 & 0 & 0 & 0 & 0 & -1 & -1 & 1 \\ 0 & 0 & 0 & 0 & 0 & 0 & 0 & 0 & 0 & 0 & 0 & 0 & 0 & 0 & -1 & -1 & 1 \\ \hline 0 & 0 & 0 & 0 & 0 & 0 & 0 & 0 & 0 & 0 & 0 & 0 & -1 & 0 & 0 & 0 & 0 \\ 0 & 0 & 0 & 0 & 0 & 0 & 0 & 0 & 0 & 1 & 0 & 0 & 0 & 0 & 0 & 0 & 0 \\ \hline 0 & 0 & 0 & 0 & 0 & 0 & 0 & 0 & 0 & 0 & 0 & -1 & 0 & 0 & 0 & 0 & 0 \\ 0 & 0 & 0 & 0 & 0 & 1 & 0 & -1 & 0 & 0 & 0 & 0 & 0 & 0 & 0 & 0 & 0 \\ \hline 0 & 0 & 0 & 0 & 0 & 0 & 1 & 0 & 0 & 0 & 0 & 0 & 0 & 0 & 0 & 0 & 0 \\ 0 & 0 & 0 & 0 & 0 & -1 & 0 & 0 & 0 & 0 & 0 & 0 & 0 & 0 & 0 & 0 & 0 \\ \hline 0 & 0 & 0 & 0 & 0 & 0 & 0 & 1 & 1 & 0 & 0 & 0 & 0 & 0 & 0 & 0 & 0 \\ 1 & 1 & 0 & 0 & 0 & 0 & 0 & 0 & 0 & 0 & 0 & 0 & 0 & 0 & 0 & 0 & 0 \\ 1 & 1 & 0 & 0 & 0 & 0 & 0 & 0 & 0 & 0 & 0 & 0 & 0 & 0 & 0 & 0 & 0 \\ \hline 0 & 0 & 0 & 1 & 1 & 0 & 0 & 0 & 0 & 0 & 0 & 0 & 0 & 0 & 0 & 0 & 0 \\ 0 & 0 & 0 & 1 & 1 & 0 & 0 & 0 & 0 & 0 & 0 & 0 & 0 & 0 & 0 & 0 & 0 \\ 0 & 0 & 0 & 0 & 0 & 0 & 0 & 0 & 0 & 0 & 0 & 0 & 0 & 0 & 0 & 0 & 0 \\ \hline 0 & 0 & 0 & 0 & 0 & 0 & 0 & 0 & 0 & 0 & 0 & 0 & 0 & 0 & 0 & 0 & 0 \\ 0 & 0 & 0 & 0 & 0 & 0 & 1 & 0 & 0 & 0 & 0 & 0 & 0 & 0 & 0 & 0 & 0 \\ 0 & 0 & 0 & 0 & 0 & 0 & 0 & 0 & 0 & -1 & 0 & 0 & 0 & 0 & 0 & 0 & 0 \end{bmatrix}$$

There is a lot of information that can be derived from that matrix. Here is an example.

Corollary 2.2 *The Hénon map contains a periodic orbit of any minimal period $p \in \mathbf{N} \setminus \{3, 5\}$.*

Proof. Let B_i be the matrix obtained from B by substituting all entries in rows corresponding to generating paths for critical edges outside the i -th component with zeroes. Equivalently, B_i is obtained from B by replacing all its entries above the $(i - 1)$ -th horizontal line and below the i -th line with zeroes. A straightforward but arduous computation shows that:

1. $\text{tr } B_5 = -1$
2. $\text{tr } B_2 B_{10} = -1$
3. $\text{tr } B_1 B_{11} B_4 B_9 = -1$
4. $\text{tr } B_8 B_1 B_{11} B_7 B_6 B_3 = -1$

5. $\text{tr } B_3 B_8 B_1 B_{11} B_7 B_6 (B_5)^k = (-1)^k$ for $k \geq 1$.

By Theorem 1.5 (part 2), H has periodic points of all minimal periods except for (possibly) 3 and 5. \square

In [28] we have shown that the periodic orbits whose existence is proved above in fact belong to the Hénon attractor. Furthermore, by using a simple argument based on the technique of Lyapunov functions we showed that in fact there are no orbits of period 3 and 5 within the attractor.

2.5.2 Area Preserving Hénon Map

The area preserving Hénon map is a homeomorphism of the plane given by the formula

$$\bar{H}(x, y) = (\cos \alpha x - \sin \alpha y + \sin \alpha x^2, \sin \alpha x + \cos \alpha y - \cos \alpha x^2),$$

where α is a parameter, in our case assumed to be $\cos^{-1} 0.24$. It is not hard to see that $|\det D\bar{H}| = 1$ at any point of the plane and hence that H is indeed an area-preserving homeomorphism. For this example, we applied the procedures described before for $\epsilon_1 = \epsilon_2 = 2/345$. One of the index pairs produced by the algorithm is shown on Figure 10. The solid dark line is the border of the set in which the index pair was searched for. The discrete representation of \bar{H} was computed as in the preceding example. The cohomology computation procedure produces the following matrix.

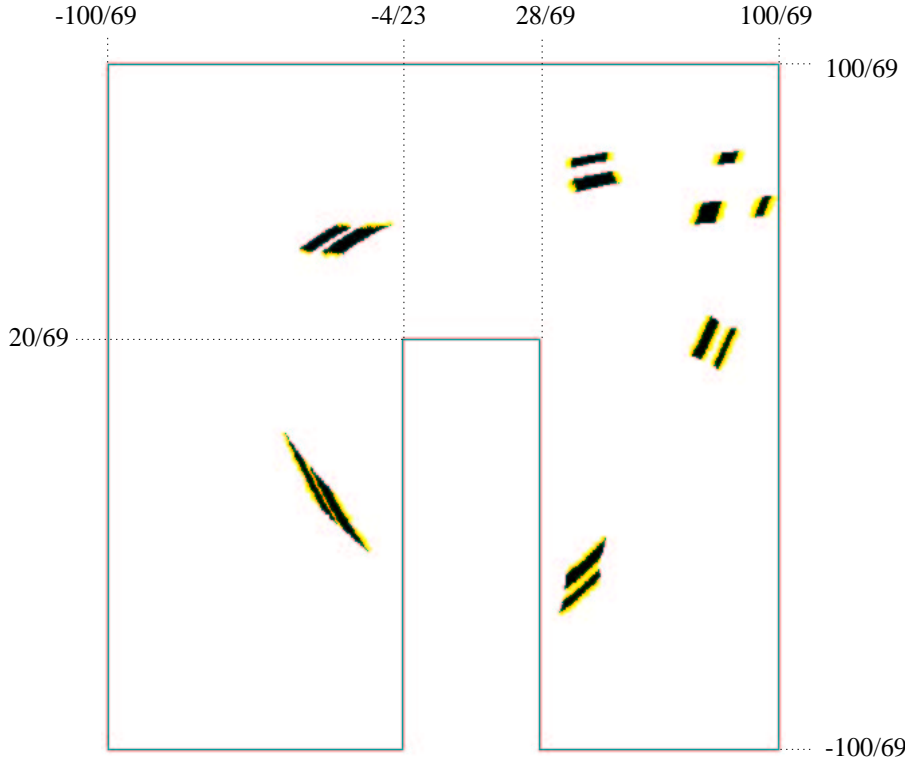


Figure 10: *An index pair for the area preserving Hénon map.*

$$B = \begin{bmatrix} 0 & 1 & 0 & 0 & 0 & 0 & 0 & 0 & 0 & 0 & 0 & 0 & 0 & 0 & 0 & 0 \\ 0 & 0 & 0 & 0 & 0 & 0 & 1 & 0 & 0 & 0 & 0 & 0 & 0 & 0 & 0 & 0 \\ 1 & 0 & 0 & 0 & 0 & 0 & 0 & 0 & 0 & 0 & 0 & 0 & 0 & 0 & 0 & 0 \\ 0 & 0 & 0 & 0 & 0 & 1 & 0 & 0 & 0 & 0 & 0 & 0 & 0 & 0 & 0 & 0 \\ 0 & 0 & 0 & -1 & 0 & 0 & 0 & 0 & 0 & 0 & 0 & 0 & 0 & 0 & 0 & 0 \\ 0 & 0 & 0 & 0 & 0 & 0 & 0 & 0 & 0 & 1 & 0 & 0 & 0 & 0 & 0 & 0 \\ 0 & 0 & 0 & 0 & 0 & 0 & 0 & 0 & 0 & 0 & 1 & 0 & 0 & 0 & 0 & 0 \\ 0 & 0 & 0 & 0 & -1 & 0 & 0 & 0 & 0 & 0 & 0 & 0 & 0 & 0 & 0 & 0 \\ 0 & 0 & 1 & 0 & 0 & 0 & 0 & 0 & 0 & 0 & 0 & 0 & 0 & 0 & 0 & 0 \\ 0 & 0 & 0 & 0 & 0 & 0 & 0 & 0 & 0 & 0 & 0 & 0 & 0 & -1 & 0 & -1 \\ 0 & 0 & 0 & 0 & 0 & 0 & 0 & 0 & 0 & 0 & 0 & 1 & -1 & 0 & 1 & -1 \\ 0 & 0 & 0 & 0 & 0 & 0 & 0 & 0 & 0 & 0 & 0 & 0 & 0 & 0 & 0 & 0 \\ 0 & 0 & 0 & 0 & 0 & 0 & 0 & 0 & 0 & 0 & 0 & 0 & 0 & 0 & 0 & 0 \\ 0 & 0 & 0 & 0 & 0 & 0 & 0 & -1 & 0 & 0 & 0 & 0 & 0 & 0 & 0 & 0 \\ 0 & 0 & 0 & 0 & 0 & 0 & 0 & -1 & 0 & 0 & 0 & 0 & 0 & 0 & 0 & 0 \\ 0 & 0 & 0 & 0 & 0 & 0 & 0 & 0 & 0 & 0 & 0 & 0 & 0 & 0 & 0 & 0 \\ 0 & 0 & 0 & 0 & 0 & 0 & 0 & 0 & -1 & 0 & 0 & 0 & 0 & 0 & 0 & 0 \\ 0 & 0 & 0 & 0 & 0 & 0 & 0 & -1 & 0 & 0 & 0 & 0 & 0 & 0 & 0 & 0 \end{bmatrix}$$

An example of a property which can be inferred from the results of the computation described above is given below.

Corollary 2.3 *The map \bar{H} has an isolated invariant set S such that there is a surjection $\bar{q} : S \rightarrow \Sigma := \prod_{i=0}^{\infty} \{0, 1\}$ such that $\bar{q} \circ \bar{H}^{19} = \sigma \circ \bar{q}$, where by σ we denote the shift map on Σ . Moreover, \bar{q} can be chosen in such a way that each periodic sequence in Σ is an image of a periodic point $x \in S$ of \bar{H}^{19} of the same least period.*

Proof. Let \bar{q} be defined as follows. Consider the map $q : S \rightarrow \Pi := \prod \{1, 2, \dots, 12\}$ defined in Section . For $x \in S$ let $q(x)_i$ be the i -th entry of $q(x)$ (recall that, by convention, we start indexing the sequence $q(x)$ with 0). Define $\bar{q}(x) := (\mu(q(x)_{19i+2}))_{i=0}^{\infty}$, where

$$\mu(a) = \begin{cases} 1 & \text{if } a = 8 \\ 0 & \text{otherwise.} \end{cases}$$

Let e_1, e_2, \dots, e_{18} be the consecutive vectors of the basis in which the matrix B is written and matrices B_i be defined as in the previous section. Let P be the matrix of the orthogonal projection onto the one-dimension space spanned by the 10-th basis vector. It is straightforward to see that

$$B_{10}B_{12}B_8B_5B_4B_6 = B_{10}B_{12}B_9B_3B_1B_2B_7B_{11}B_{12}B_8B_5B_4B_6 = P.$$

Let $B'_0 = B_{10}B_{12}B_8B_5B_4B_6$ and $B'_1 = B_{10}B_{12}B_9B_3B_1B_2B_7B_{11}B_{12}B_8B_5B_4B_6$. Put $\bar{B}_1 = B'_0B'_1$ and $\bar{B}_0 = B'_1B'_0$. Any product of \bar{B}_0 and \bar{B}_1 is equal to P and therefore has the trace of 1. By Theorem 1.5 (part 2), any periodic sequence in Π which can be obtained by concatenating a finite number of sequences (each of them of length 19)

$$(10, 12, 8, 5, 4, 6, 10, 12, 9, 3, 1, 2, 7, 11, 12, 8, 5, 4, 6)$$

and

$$(10, 12, 9, 3, 1, 2, 7, 11, 12, 8, 5, 4, 6, 10, 12, 8, 5, 4, 6)$$

and repeating the concatenation indefinitely is an image of a periodic point of \bar{H} of the same least period. Similarly, any infinite concatenation of these sequences is in

the image of S under q . The statement which we want to prove is nothing but a restatement of that using \bar{q} rather than q . \square

Chapter 3

An Application to Time Series Analysis

This chapter describes an application of the techniques presented before to a dynamical system modeled using time series data coming from the magnetoelastic ribbon experiment. A detailed description of that experiment can be found in Section 3.2.3. The results of our computation carry some information about the diversity of time series data one can expect to collect by running the same experiment for varying initial conditions. Our method is robust under perturbation (see [17], [27], [28] for more precise statements), and therefore is not as sensitive to measurement errors or inevitable inaccuracies of the experimental setup as other approaches.

3.1 Experimental Assumptions and Notation

We shall present in this section a series of assumptions concerning the physical system and the experimental measurements, comments concerning these assumptions and some of their simplest consequences. In an experimental setting, we cannot hope to verify these assumptions, but we present them as a check to the experimentalist.

The most fundamental of the assumptions is that the physical system can be modeled by a continuous map $f : X \times \Lambda \rightarrow X$. One can look at f as a parameterized family of maps of X into itself. By f_λ we shall denote the map $f(\cdot, \lambda) : X \rightarrow X$. By an *experiment* we mean a sequence $\{x_j, \lambda_j\}_{j=0}^J$ of points of X and parameter values in $\Lambda_E \subset \Lambda$ satisfying $x_{j+1} = f_{\lambda_j}(x_j)$. In practice all experiments are finite but sometimes

it will be convenient to use the concept of an infinite experiment, i.e. one in which $J = \infty$.

An important observation at this point is that we allow the parameter values λ_j to vary randomly. This appears to be the only physically realistic assumption that is possible. The experimentalist can never have complete control over the experiment or exactly choose parameter values. Therefore, the only constraint that we impose on the parameter values is that during the experiment they can be controlled to lie within $\Lambda_E \subset \Lambda$. An implication of this is that if we are given a point $x \in X$ then after one iteration all we can assume is that it lies in

$$f_{\Lambda_E}(x) := f(\{x\} \times \Lambda_E) \subset X.$$

A second reason for insisting that parameter values should be allowed to vary randomly over some Λ_E is that physically it is impossible to sample at precise time intervals. Therefore, if one views the sampling as choosing points along a trajectory of f_τ , then small uncontrolled changes in the time of sampling can be thought of as being equivalent to choosing points along a trajectory obtained by the sequence of maps $f_{\tau_0}, f_{\tau_1}, f_{\tau_2}$, etc. By continuity with respect to time these maps are small perturbations from f_τ and therefore can be incorporated into Λ_E assuming the space of perturbations Λ is chosen large enough.

The process of measuring an experiment inherently involves errors. Therefore, we choose to model the measurements as multivalued maps. Namely, by a *measurement* we shall denote a multivalued map, assigning an interval $\theta(x) = [a_x, b_x]$ to every point $x \in X$. Thus, we chose the measurement tolerance error $b_x - a_x$ to depend only on x , not on time. In order for the experimental data to have any meaning there must be some amount of continuity in the measurement map. If not, then arbitrarily small changes in the physical system could result in instantaneous arbitrarily large changes in measurements. We choose to impose this restriction by assuming that a

hypothetical ‘true’ measurement, $\gamma(x) \in \mathbf{R}$ exists even if it cannot be performed. More precisely, we assume that γ is a continuous function being a selector of θ , i.e. such that $\gamma(x) \in \theta(x)$ for each $x \in X$.

We are now in position to define a time series.

Definition 3.1 *A time series data is a sequence of real numbers $(u_j)_{j=0}^J$ for which there exists an experiment $E = \{x_j, \lambda_j\}_{j=0}^J$ such that $u_j \in \theta(x_j)$. The time series is sampled from $A \subset X$ if, additionally, $x_j \in A$ for all $0 \leq j \leq J$.*

Observe that the relationship which is required to hold between the time series data and the ‘true’ physical process is that, pointwise,

$$|u_j - \gamma(x_j)| \leq b_{x_j} - a_{x_j}$$

One of the consequences of the above definitions is that if the system is in state x at some moment in time then the next n measurements of its state may be $\theta(x_1), \theta(x_2), \dots, \theta(x_n)$, where x_1, x_2, \dots, x_n are such that $x_{i+1} \in f_{\Lambda_E}(x_i)$ for $i = 1, 2, \dots, n-1$ and $x_1 = x$. This motivates the following definition which introduces a map capturing all possible measurements for up to n time steps.

Definition 3.2 *The generalized reconstruction map is a multivalued map of X into \mathbf{R}^n defined as follows.*

$$M_n(x) := \bigcup_{(x_1, x_2, \dots, x_n) \in T_n(x)} \theta(x_1) \times \theta(x_2) \times \dots \times \theta(x_n),$$

where

$$T_n(x) = \left\{ (x_1, x_2, \dots, x_n) \in X^n : x_1 = x \text{ and there exist } \lambda_1, \lambda_2, \dots, \lambda_{n-1} \in \Lambda_E \text{ such that } x_{i+1} = f_{\lambda_i}(x_i) \text{ for } i = 1, 2, \dots, n-1 \right\}.$$

Clearly, the range of M_n contains all points which can be achieved through experimentation.

In practice the points which come from experiments usually are not spread out over the whole range of M_n . Instead they tend to accumulate around a much smaller region of \mathbf{R}^n . We shall assume that this kind of behavior is a result of the existence of a set A such that $f_{\Lambda_E}(x) \subset A$ for any $x \in A$ and the time series data reflects the dynamics of f on A in the sense which will be defined later. Our goal is to describe the dynamics of f on A .

Clearly, f induces a multivalued dynamical system E_n on $O_n = M_n(A)$ defined by

$$E_n(y) := \left\{ v \in O_n : \begin{array}{l} \exists x \in A \text{ such that } y \in M_n(x), \\ \exists \lambda \in \Lambda_E \text{ such that } v \in M_n(f_\lambda(x)) \end{array} \right\}.$$

Given only the constraints described above, E_n represents the optimal knowledge of the dynamics on A as viewed through an n -dimensional delay reconstruction. This can be seen by realizing that given y a vector obtained from n consecutive data points, $y = (u_j, u_{j+1}, \dots, u_{j+n-1})$, the best safe prediction that can be made concerning u_{j+n} is that $(u_{j+1}, \dots, u_{j+n}) \in E_n(y)$. Any set smaller than $E_n(y)$ fails to contain a possible image point. Unfortunately, it is impossible in practice to compute E_n . Therefore, we weaken our expectations concerning the dynamics which will be studied on \mathbf{R}^n .

Definition 3.3 *A multivalued map $F : D \rightarrow D$ (where $D \subset \mathbf{R}^n$) is an envelope of f if, for some true measurement γ , the following two conditions are satisfied for any sequence of parameter values in $\Lambda_E \subset \Lambda$ ($\lambda_1, \lambda_2, \dots, \lambda_n$).*

1. $\Gamma_{\lambda_1, \lambda_2, \dots, \lambda_{n-1}}^\gamma(A) \subset D$, where

$$\Gamma_{\lambda_1, \lambda_2, \dots, \lambda_{n-1}}^\gamma(x) = \left(\gamma(x), \gamma(f_{\lambda_1}(x)), \dots, \gamma(f_{\lambda_{n-1}} \circ f_{\lambda_{n-2}} \circ \dots \circ f_{\lambda_1}(x)) \right)$$

2. *The diagram*

$$\begin{array}{ccc} A & \xrightarrow{f_{\lambda_1}} & A \\ \downarrow \Gamma_{\lambda_1, \lambda_2, \dots, \lambda_{n-1}}^\gamma & & \downarrow \Gamma_{\lambda_2, \lambda_3, \dots, \lambda_n}^\gamma \\ D & \xrightarrow{F} & D \end{array}$$

upper-semicommutates i.e., for every $x \in A$,

$$\Gamma_{\lambda_2, \dots, \lambda_n}^\gamma \circ f_{\lambda_1}(x) \in F \circ \Gamma_{\lambda_1, \lambda_2, \lambda_3, \dots, \lambda_{n-1}}^\gamma(x).$$

One of our fundamental assumptions will be that our model of the system constructed based on the time series data is an envelope of f . The following two propositions are straightforward.

Proposition 3.1 E_n is an envelope for f .

Proposition 3.2 If $F : D \rightarrow D$ is a multivalued map such that $E_n(y) \cap D \subset F(y)$ for all $y \in D$ then F is an envelope for f provided that for some true measurement γ

$$\Gamma_{\lambda_1, \lambda_2, \dots, \lambda_{n-1}}^\gamma(A) \subset D$$

for any $\lambda_1, \lambda_2, \dots, \lambda_{n-1} \in \Lambda_E$.

3.2 Implementation

In this section, $(u_j)_{j=0}^J$ stands for a time series sampled from $A \subset X$. Clearly, we cannot ensure that the time series is sampled from A if it was obtained from a physical experiment. However physical systems quite often possess global attractors and their positively invariant neighborhoods are a natural choice for A . In such cases, the state of the system must eventually enter A during the experiment and it never leaves A afterwards. Thus, any time series can be transformed to one sampled from A by discarding some number of its initial entries. Again, it is not possible to tell how many entries have to be discarded. In practice, we discard so many that the resulting series yields a clean reconstruction of the system, with relatively small values of each cube in \mathcal{D} .

In what follows, $\{x_j, \lambda_j\}_{j=0}^J$ is the experiment giving rise to (u_j) , i.e. such that $u_j \in \theta(x_j)$. We shall assume that $J < \infty$.

3.2.1 Modeling of the System

Define

$$\Sigma_n := \{(u_j, u_{j+1}, \dots, u_{j+n-1}) : j \in \{0, 1, \dots, J-n\}\}.$$

By \mathcal{D} we shall denote the set of all grid cubes in Ω intersected by Σ_n . Let $T_n : \Sigma_n \rightarrow \mathbf{R}^n$ be the multivalued map defined by

$$T_n(v_0, v_1, \dots, v_{n-1}) = \left\{ (u_{j+1}, u_{j+2}, \dots, u_{j+n}) : 0 \leq j \leq J-n, \right. \\ \left. (v_0, v_1, \dots, v_{n-1}) = (u_j, u_{j+1}, \dots, u_{j+n-1}) \right\}.$$

The map T_n is a natural representation of the dynamics of the time series data. However, it is defined on a finite set of points Σ_n . This set certainly neither covers the entire range that can be achieved by experimentation nor possesses any interesting topology. Therefore, a fundamental problem which we are facing at this point is how to extend that map to a neighborhood of Σ_n so that the extension is likely to be an envelope of the physical system f . We decided to take a straightforward approach to that problem: for each grid cube K we make its image be a convex neighborhood containing all points $(u_{j+1}, u_{j+2}, \dots, u_{j+n})$ such that the point defined by the preceding window in the time series, i.e. $(u_j, u_{j+1}, \dots, u_{j+n-1})$, is in K . The definitions are given below.

Define the multivalued map $\mathcal{T}_n : \Omega \rightarrow \Omega$ by

$$\mathcal{T}_n(K) = \{L \in \Omega : T_n(K \cap \Sigma_n) \cap L \neq \emptyset\}.$$

Definition 3.4 A map $\mathcal{G} : \Omega \rightarrow \Omega$ is said to be consistent with the time series data if the following condition is satisfied:

$$T_n(K \cap \Sigma_n) \subset |\mathcal{G}(K)| \quad \text{for each } K \in \Omega.$$

Obviously, \mathcal{T}_n is consistent with the time series data.

However, \mathcal{T}_n is not ‘large’ enough for our purposes. The fact that there is only one point of Σ_n in a grid cube does not necessary mean that the image of that cube (or even that point) under the generalized reconstruction map (cf Definition 3.2) intersects only one grid cube. To make our approach completely reliable, we would have to make sure that our model of the system is its valid envelope. Since we cannot have complete knowledge about the physical system, this is impossible in practice. We do what seems to be a reasonably good try. In order to get a value of a cube under the model map we start with the smallest convex representable set containing $\mathcal{T}_n(K)$ and then enlarge it by applying the ‘ o ’ operation (defined in Section 2.1). More precisely, for a set $\mathcal{A} \subset \Omega$ and a nonnegative integer δ let \mathcal{B}_δ be defined recursively as follows:

$$\mathcal{B}_0(\mathcal{A}) := \mathcal{A}, \quad \mathcal{B}_{\alpha+1}(\mathcal{A}) := o(\mathcal{B}_\alpha(\mathcal{A})).$$

By $r(\mathcal{A})$ we shall denote the representation of the smallest representable convex set (i.e. either empty or of the form $[l_1\epsilon, k_1\epsilon] \times [l_2\epsilon, k_2\epsilon] \times \dots \times [l_n\epsilon, k_n\epsilon]$, where $l_1, k_1, l_2, k_2, \dots, l_n, k_n$ are integers such that $l_i < k_i$ for $i = 0, 1, \dots, n$) containing $|\mathcal{A}|$. The discrete model of the system will be defined by the multivalued map \mathcal{F}_n^δ given by (see Figure 11 for an illustration)

$$\mathcal{F}_n^\delta(K) = \mathcal{B}_\delta(r(\mathcal{T}_n(K))).$$

The multivalued map $F_n^\delta : D \rightarrow D$, where $D = |\mathcal{D}|$ (recall that \mathcal{D} is the set of grid cubes containing sample points from the time series), which will represent the

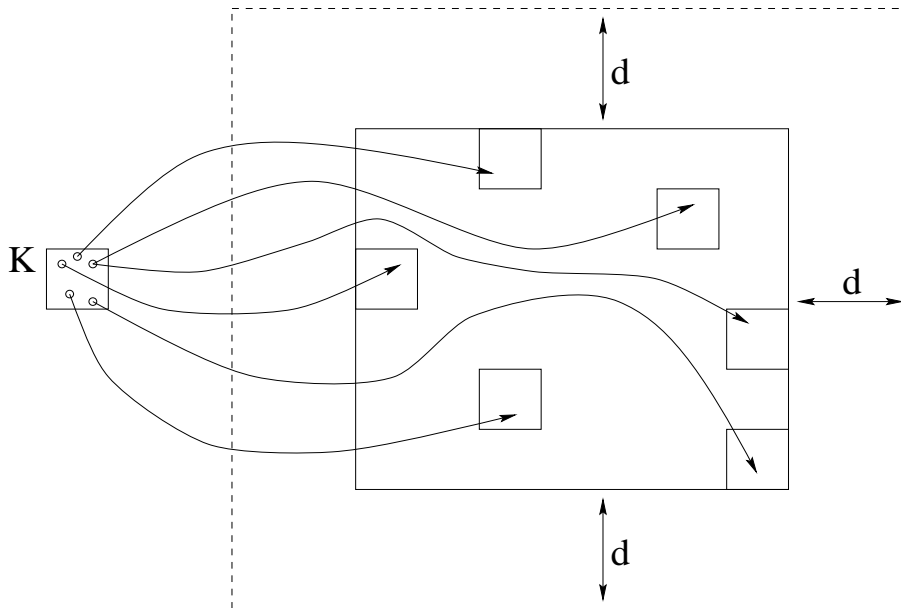


Figure 11: *Construction of \mathcal{F}_n^δ . Arrows indicate the action of T_n , small circles are points of $K \cap \Sigma_n$ and $d = \delta\epsilon$. The large dashed rectangle is the set represented by $\mathcal{F}_n^\delta(K)$.*

physical system in the reconstruction coordinates is given by

$$F_n^\delta(x) := D \cap \bigcap_{K \in \Omega: x \in K} |\mathcal{F}_n^\delta|(x).$$

The two most important factors influencing the choice of δ are as follows.

1. It should be large enough so that the multivalued map represented by \mathcal{F}_n^δ (i.e. the map F_n^δ) is (in practice, is likely to be) an envelope of f .
2. δ should not be too large – otherwise it would not provide enough information to infer anything interesting about the dynamics of f .

In practice, it is easy to verify if the chosen δ satisfies condition 2 – one simply runs the procedure described in the following section for \mathcal{F}_n^δ and, if it does not produce expected results, attempts to decrease δ . On the other hand, condition 1 is impossible to verified in practice without a doubt. We take a pragmatic approach and require

that the following condition which is obviously necessary (but not always sufficient) is satisfied. For any set of grid cubes in \mathcal{D} with nonvoid intersection, the intersection of their images under \mathcal{F}_n^δ is also nonvoid. An alternative criterion for F_n^δ to be an envelope of f , based on the modulus of continuity of B_n , is given in Section 3.3. It is much more elegant from theoretical standpoint. However, it is much harder to verify in practice for an experimental time series. In fact, we were not able to do that for the magnetoelastic ribbon time series data described later on since our time series was not long enough and of good enough quality.

3.2.2 Symbolic Dynamics from the Model

The procedure for isolating neighborhoods described in Section 2.3 can be applied for the map $\mathcal{F} = \mathcal{F}_n^\delta$, yielding a set $\mathcal{N} \subset \Omega$ such that $\mathcal{N} = \text{Inv}_{\mathcal{F}o}(\mathcal{N})$. Having empty image, grid cubes outside \mathcal{D} do not have forward trajectories and therefore cannot belong to \mathcal{N} . Hence $\mathcal{N} \subset \mathcal{D}$. Let $N = |\mathcal{N}|$, $N_0 = \text{bd}_D N = \text{cl}N \cap \text{cl}(D \setminus N)$ and $F = F_n^\delta$. Assume that $F_n^\delta(N_0) \cap N \subset N_0$.

By Z we shall define the union of all connected components of $|\mathcal{D} \setminus \mathcal{N}|$ not intersected by $F(N_0)$. Let $\{B_1, B_2, \dots, B_m\}$ and $\{C_0, C_1, \dots, C_m\}$ be decompositions of N and $\text{cl}((D \setminus Z) \setminus N)$ (respectively) into pairwise disjoint compact sets. We shall assume that those decompositions are such that only pairs of consecutive sets in $C_0, B_1, C_1, B_2, \dots, B_m, C_m$ have nonempty intersection. Note that the sets B_i and C_j are not uniquely determined by \mathcal{D} and \mathcal{N} (see Figure 12 for an example).

For $i = 0, 1, \dots, m$ let $B_i^+ = B_i \cap C_{i+1}$ and $B_i^- = B_i \cap C_i$. By assumptions about D and N , F maps B_i^* into the union of C_i 's (for $* \in \{+, -\}$). By I_i^* we shall denote the set of all indices j for which $F(B_i^*)$ intersects C_j . For two sets of integers J_1, J_2 we shall use the notation $J_1 < J_2$ to indicate that each element of J_1 is strictly less

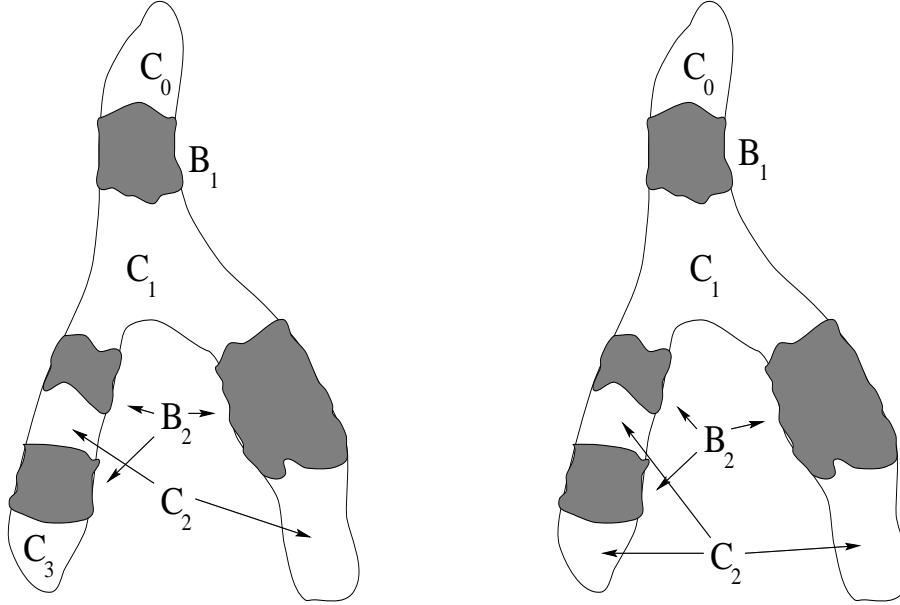


Figure 12: *Examples of partitions of N and $\text{cl}(D \setminus N)$ into disjoint compact sets. The inverted-Y shaped curve bounds D and the set N is shaded.*

than any element of J_2 (equivalently, $\max J_1 < \min J_2$). The set S_i is defined as the set of indices lying ‘between’ J_1 and J_2 . More precisely,

$$S_i = \begin{cases} (\max I_i^+, \min I_i^-] \cap \mathbf{N} & \text{if } I_i^+ < I_i^- \\ (\max I_i^-, \min I_i^+] \cap \mathbf{N} & \text{if } I_i^- < I_i^+ \\ \emptyset & \text{otherwise.} \end{cases}$$

By B we shall denote the *connectivity transition matrix* i.e. the $m \times m$ matrix $[b_{ij}]$ whose coefficients are given by

$$b_{ij} = \begin{cases} 1 & \text{if } j \in S_i \\ 0 & \text{otherwise.} \end{cases}$$

For the example shown in Figure 13, $I_1^- = \{1\}$, $I_1^+ = \{2\}$, $I_2^- = \{0, 1\}$, $I_2^+ = \{3\}$, $I_3^- = \{0\}$ and $I_3^+ = \{1\}$. Thus, $S_1 = \{2\}$, $S_2 = \{2, 3\}$ and $S_3 = \{1\}$. Hence the transition matrix is

$$\begin{bmatrix} 0 & 1 & 0 \\ 0 & 1 & 1 \\ 1 & 0 & 0 \end{bmatrix}$$

The following definition will play a crucial role in our way of describing the dynamics of the time series in terms of symbols.

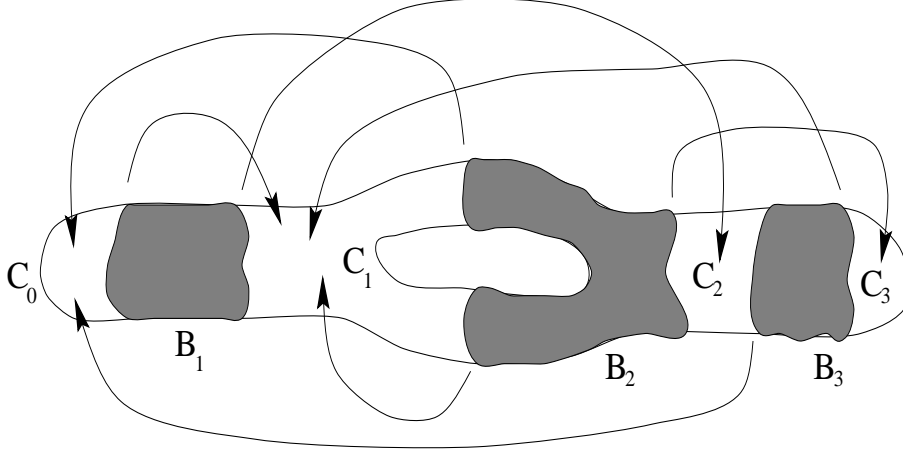


Figure 13: *An example partition of D and the way F acts on it (indicated by the arrows).*

Definition 3.5 *A sequence $(i_j)_{j=0}^{\infty}$ of numbers in $\{1, 2, \dots, m\}$ is called admissible if and only if the following two properties are satisfied.*

1. *There is a path $\sigma : [0, 1] \rightarrow A$ such that for all parameter values $\mu_1, \mu_2, \dots, \mu_{n-1} \in \Lambda_E$, $\Gamma_{\mu_1, \mu_2, \dots, \mu_{n-1}}^{\gamma} \circ \sigma$ is a path starting in C_{i_0-1} and ending in C_{i_0} ; γ is a true measurement satisfying the conditions in Definition 3.3*
2. *For each j , the entry of B in the i_j -th row and i_{j+1} -th column is nonzero.*

Let P_i be the projection of B_i onto the first coordinate, i.e. the set of all $x \in \mathbf{R}$ for which there exist y_1, y_2, \dots, y_{n-1} such that the point $(x, y_1, y_2, \dots, y_{n-1})$ belongs to B_i . We have the following theorem.

Theorem 3.1 *Let $(i_j)_{j=0}^{\infty}$ be an admissible sequence. For any sequence of parameters $\{\lambda_j\}_{j=0}^{\infty} \subset \Lambda_E$ there exists an experiment $\{x_j, \lambda_j\}_{j=0}^{\infty}$ sampled from A such that $\theta(x_j) \cap P_{i_j} \neq \emptyset$ for all $j \in \mathbf{Z}^+$.*

Proof. Define $\Gamma_j = \Gamma_{\lambda_j, \lambda_{j+1}, \dots, \lambda_{j+n-1}}^{\gamma}$. Let $\sigma : [0, 1] \rightarrow A$ be a path as in Definition 3.5,1., i.e. such that $\Gamma_0 \circ \sigma(0) \in C_{i_0-1}$ and $\Gamma_0 \circ \sigma(1) \in C_{i_0}$. We shall show that there

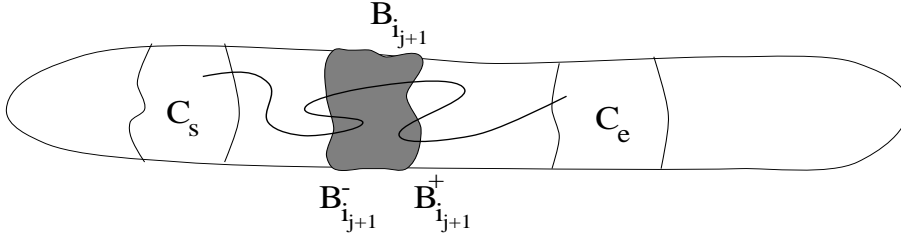


Figure 14: *The inductive step of the proof of Theorem 3.1. The path $\sigma_{j+1}|_{L_j}$ runs from C_s to C_e and therefore crosses $B_{i_{j+1}}$.*

exists a sequence of intervals

$$[0, 1] \supset L_0 \supset L_1 \supset \dots$$

satisfying the following conditions.

(*) The math $\sigma_j := \Gamma_j \circ f_{\lambda_{j-1}} \circ f_{\lambda_{j-2}} \circ \dots \circ f_{\lambda_0} \circ \sigma$ maps the interval L_j into B_{i_j} , sending one of its endpoints into $B_{i_j}^+$ and the other - into $B_{i_j}^-$.

Having proven the above, the assertion of Theorem 3.1 follows easily: for any $u \in \bigcap_{j=0}^{\infty} L_j$, the sequence $\{f_{\lambda_{j-1}} \circ f_{\lambda_{j-2}} \circ \dots \circ f_{\lambda_0}(\sigma(u)), \lambda_j\}$ is an experiment satisfying the required properties. We shall construct intervals L_j satisfying the condition (*) using induction on j .

For $j = 0$, let

$$L_0 := \left[\max \sigma^{-1}(B_{i_0}^-), \min\{t \in \sigma^{-1}(B_{i_0}) : t > \max \sigma^{-1}(B_{i_0}^-)\} \right].$$

Assume that L_j has been defined so that the condition (*) holds. Definition 3.3 and assumptions about how F acts on B_i^* 's imply that the map $\Gamma_{j+1} \circ f_j \circ f_{j-1} \circ \dots \circ f_0 \circ \sigma$ maps one of the endpoints of the interval L_j into C_s and the other into C_e where $s \in I_{i_j}^+$ and $e \in I_{i_j}^-$. Thus (see Figure 14) the path $\sigma_{j+1}|_{L_j}$ has to cross $B_{i_{j+1}}$. In particular, this means that there exists an interval $L_{j+1} \subset L_j$ such that σ_{j+1} maps L_{j+1} into $B_{i_{j+1}}$, one of its endpoints into $B_{i_{j+1}}^+$ and the other - into $B_{i_{j+1}}^-$. \square

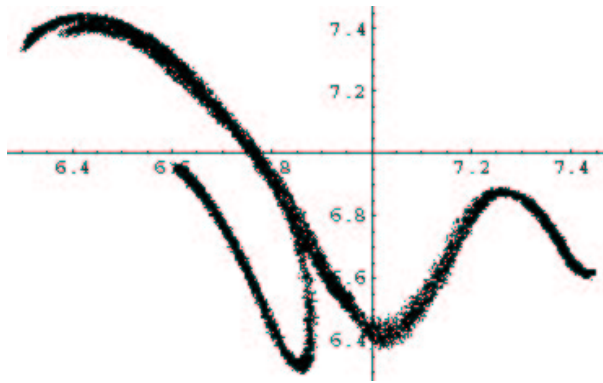


Figure 15: *The reconstruction plot for the magnetoelastic ribbon time series data*

3.2.3 Analysis of Magnetoelastic Ribbon Experiment

The magnetoelastic ribbon is a thin strip of material with the property that its Young's modulus varies with the strength of an applied magnetic field. A region of uniform magnetic field was created by the use of three Helmholtz coils. The ribbon was placed in the uniform magnetic field, and clamped from the bottom. The ribbon and Helmholtz coils were encased in a Plexiglass box. The box was placed upon a vibration isolation table, and the entire apparatus was in a temperature-controlled, sealed room. Thus environmental effects were minimized. Nevertheless, the system was extremely sensitive, and thus a significant amount of error needed to be taken into account when doing the calculations. An oscillating magnetic field was applied vertically. When the magnetic field strength is within a certain range, the ribbon will buckle under its own weight. Under these conditions, the ribbon will oscillate back and forth as its stiffness changes. Depending upon the strength of the applied uniform field, and the strength and frequency of the applied oscillating field, as well as the physical characteristics of the ribbon, the motion of the ribbon may exhibit a wide variety of different behaviors. Due to the nonlinear relationship between Young's modulus and the strength of the applied field, the motion of the ribbon may



Figure 16: *The set D , consisting of cubes in \mathcal{D} , i.e. those whose coordinates are pairs of consecutive numbers in the time series*

be chaotic. The position of the ribbon once per driving period was investigated.

The data set consisted of 100,000 consecutive data points $\{v_n \mid n = 1, \dots, 100,000\}$ taken from voltage readings on the photonic sensor, sampled at the drive frequency of 1.2 Hz. The voltage readings were measured up to 10^{-3} volts. In our analysis, we used 30,000 data points $\{v_n : 30,000 \leq n \leq 60,000\}$ and chose the reconstruction dimension of 2, producing the reconstruction plot shown in Figure 15.

The combinatorial representation of the domain D of the envelope of the reconstructed dynamical system consists of grid squares intersecting the reconstruction plot. For the time series data described here, we chose the side of a grid square to be $\epsilon = 0.0106$. The squares which are in \mathcal{D} , the representation of D , are shown shaded in Figure 16

Figure 17 depicts the decomposition of the set $|\mathcal{N}|$ into disjoint and compact B'_i s and the decomposition of $|\mathcal{D} \setminus \mathcal{N}|$ into disjoint and compact sets C_i . The cubes contained in D which are adjacent to a cube in \mathcal{N} but do not belong to \mathcal{N} are the

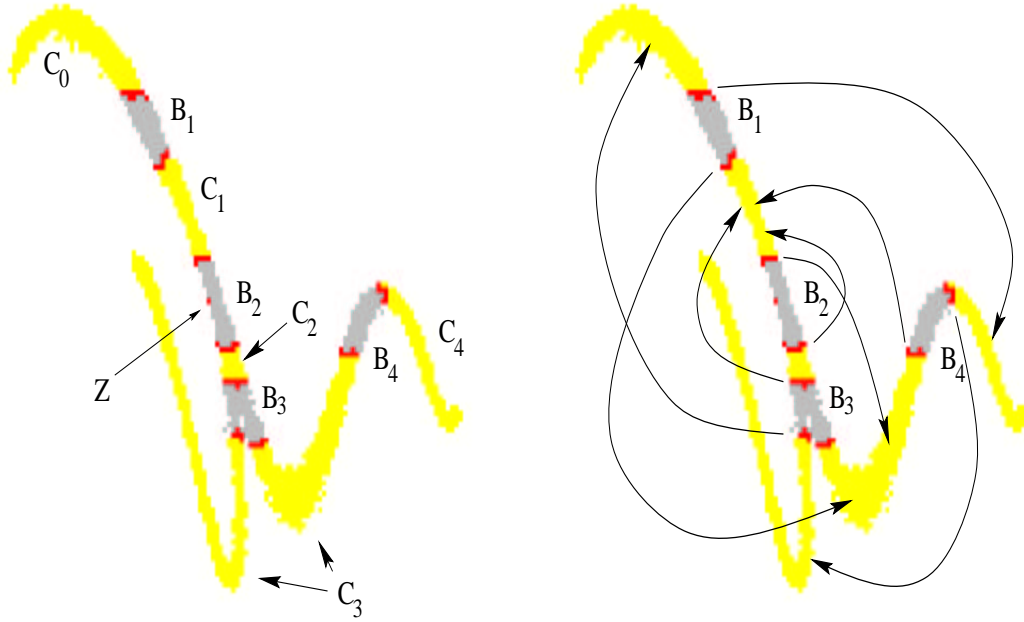


Figure 17: A partition of D into C_i 's and B_i 's (left) and the way B_i 's are mapped into C_i 's by the model F (right)

darkest. The dark square in the middle of B_2 is in fact contained in Z , i.e. it is not intersected by images of any of the dark shaded squares. The multivalued map modeling the dynamics of the time series was constructed as described in the previous section. The transition matrix for our system (see Figure 17) turns out to be

$$A = \begin{bmatrix} 0 & 0 & 0 & 1 \\ 0 & 1 & 1 & 0 \\ 1 & 0 & 0 & 0 \\ 0 & 1 & 1 & 0 \end{bmatrix}.$$

Let e be the maximum measurement error on A , i.e. the supremum of the lengths of intervals $\theta(x)$ over all $x \in A$. The result of the above computation and Theorem 3.1 imply that the physical system exhibits chaotic dynamics and sensitive dependence on initial conditions in the sense stated by the following theorem.

Theorem 3.2 *Assume that:*

1. *The multivalued map F used for the transition matrix computation is indeed an envelope for the physical system f*
2. *There is a path $\sigma : [0, 1] \rightarrow A$ such that for all parameter values $\mu_1, \mu_2, \dots, \mu_{n-1} \in \Lambda_E$ and some true measurement γ satisfying the conditions in Definition 3.3, $\Gamma_{\mu_1, \mu_2, \dots, \mu_{n-1}}^\gamma \circ \sigma$ is a path starting in C_1 and ending in C_2 .*

Then, no matter how the parameters evolve in time, for any binary sequence $(\alpha_i)_{i=0}^\infty$ with the property that there is at most one ‘1’ in each quadruple of consecutive symbols there is a time series data $(u_i)_{i=0}^\infty$ such that

$$u_i \in \begin{cases} [-\infty, a + e] & \text{if } \alpha_i = 0 \\ [b - e, \infty] & \text{if } \alpha_i = 1, \end{cases}$$

where a and b are as on Figure 18

Proof. Any sequence $(i_j)_{j=0}^\infty$ being a concatenation of strings ‘2’ and ‘2314’ is an admissible sequence. Therefore, for the binary sequence (α_j) satisfying the assumptions of the theorem, substituting each ‘0001’ with ‘2314’ and each binary symbol which is not a part of a ‘0001’ by ‘2’ yields an admissible sequence. By Theorem 3.1, for any sequence of parameter values (λ_j) from Λ_E there is an experiment $\{x_j, \lambda_j\}_{j=0}^\infty$ such that $\theta(x_j)$ intersects the projection of B_{i_j} onto the x-axis. It is easy to see that the experiment $\{x_{j+3}, \lambda_{j+3}\}$ gives rise to a time series with the required properties. \square

3.3 Modulus of Continuity and envelopes

In this section we state a sufficient condition for a multivalued map to be an envelope for f in terms of the *modulus of expansion of E_n* , i.e. the function

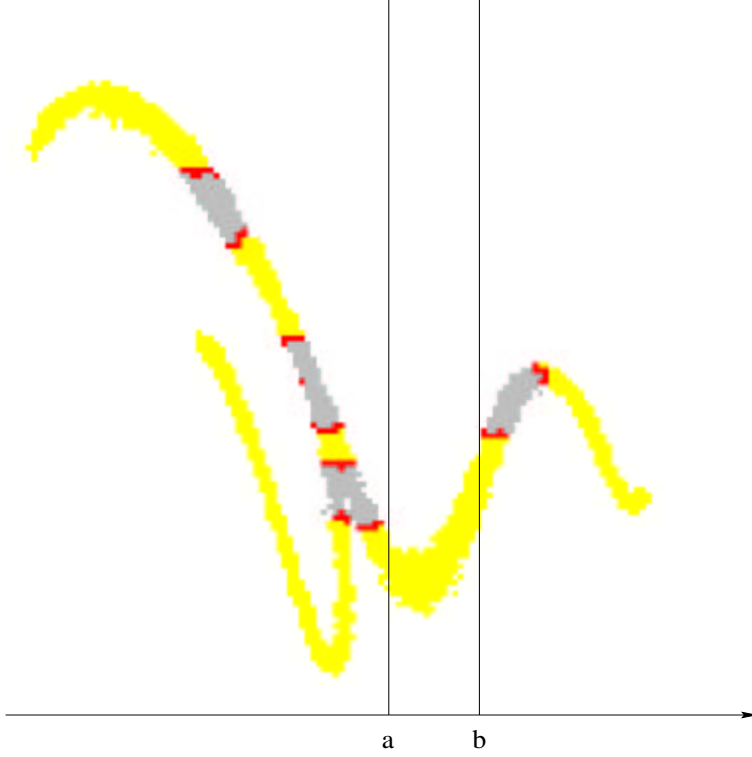


Figure 18: a and b : a is the rightmost point of the projection of B_3 and b - the leftmost point of the projection of B_4

$\epsilon : [0, \infty) \rightarrow [0, \infty)$ defined by

$$\epsilon(\delta) := \sup \left\{ \text{dist}(w_1, w_2) \mid \begin{array}{l} \exists v_1, v_2 \in O_n \text{ dist}(v_1, v_2) \leq \delta, \\ w_1 \in E_n(v_1), w_2 \in E_n(v_2) \end{array} \right\}.$$

Proposition 3.3 *Let $F : D \rightarrow D$, $D \subset \mathbf{R}^n$ be a multivalued map and $\delta > 0$ a fixed number. If the first condition of Definition 3.3 is satisfied and:*

1. $D \subset \bigcup_{\eta \in \Sigma_n} B_\delta(\eta)$,
2. $\forall \eta \in \Sigma_n \forall \eta' \in B_\delta(\eta) D \cap B_{\epsilon(\delta)}(T(\eta)) \subset F(\eta')$,
3. *the time series is sampled from A ,*

then F is an envelope of f .

Proof. Let $y \in D$. There exists $\eta \in \Sigma_n$ such that $\text{dist}(y, \eta) \leq \delta$. By the definition of the modulus of expansion (notice that $T(\eta) \in E_n(\eta)$ since the time series is sampled in A),

$$E_n(y) \cap D \subset B_{\epsilon(\delta)}(T(\eta)) \cap D \subset F(y).$$

By Proposition 3.2, the proof is finished. \square

Let us note that, in practice, the requirement that the experimental data set approximates a sufficiently large portion of D should be satisfied if the experiment is run for a sufficiently long time or sufficiently many times. Unfortunately, there is no *a priori* method for determining these times. The second hypothesis is also not rigorously verifiable in practice, but for reasonable physical systems one expects that using sufficiently many data points one can obtain a reasonable approximation to the expansion rates. In fact, approximations of this form are by now standard in the analysis of time series [1].

Bibliography

- [1] H. Abarbanel, *Analysis of Observed Chaotic Data*, Springer 1996.
- [2] R.F.Brown, *The Lefschetz Fixed Point Theorem*, Scott, Foresman and Company, Glenview, IL, London 1971.
- [3] M.M.Cohen, *A Course in Simple-Homotopy Theory*, Springer-Verlag New York Inc, 1973.
- [4] C.Conley, *Isolated Invariant Sets and the Morse Index*, CBMS Regional Conf. Ser. in Math. **38**, AMS, Providence, R.I., 1976.
- [5] T.H.Cormen, C.E.Leiserson and R.L.Rivest, *Introduction to Algorithms*, The MIT Press & McGraw Hill Book Company 1989.
- [6] Z.Galias and P.Zgliczynski, *Computer assisted proof of chaos in the Lorenz equations*, *Physica D* **115** (1998), 165-188.
- [7] P.J.Giblin, *Graphs, Surfaces and Homology*, John Wiley & Sons, New York, 1997.
- [8] M.Hénon, *A two-dimensional mapping with a strange attractor*, *Comm.Math.Phys.* **50** (1976), 69-77.
- [9] T.Kaczyński and M.Mrozek, *Stable Index Pairs for Discrete Dynamical Systems*, *Bulletin Canadian Math. Soc.*, **40**(1997), 448–455.

- [10] T.Kaczyński and M.Mrozek, *Conley index for discrete multivalued dynamical systems*, Topology Appl. **65** (1995), 83–96.
- [11] W.S.Massey, *Singular Homology Theory*, Springer-Verlag New York, 1980.
- [12] K.Mischaikow and M.Mrozek, *Isolating Neighborhoods and Chaos*, Japan Journal of Industrial and Applied Mathematics, **12** (1995), 205–236.
- [13] K.Mischaikow and M.Mrozek, *Chaos in the Lorenz Equations: a Computer Assisted Proof*, Bull.AMS **32** (1995), 66–72.
- [14] K.Mischaikow and M.Mrozek, *Chaos in the Lorenz Equations: a Computer Assisted Proof. Part II: details*, Mathematics of Computation, **67**(1998), 1023-1046.
- [15] K.Mischaikow, M.Mrozek, J.Reiss and A.Szymczak, *From time series to symbolic dynamics: an algebraic topological approach*, preliminary version.
- [16] K.Mischaikow, M.Mrozek, J.Reiss and A.Szymczak, *Construction of symbolic dynamics from time series*, Phys.Rev.Let., to appear.
- [17] K.Mischaikow, M.Mrozek and A.Szymczak, *Chaos in the Lorenz Equations: a Computer Assisted Proof. Part III: Classical Parameter Values*, in preparation.
- [18] M.Mrozek, *Leray Functor and Cohomological Conley Index for Discrete Dynamical Systems*, Trans. AMS **318** (1990).
- [19] H.-O.Peitgen, H.Jurgens and D.Saupe, *Chaos and Fractals: New Frontiers of Science*, Springer-Verlag New York Inc. 1992.
- [20] J.W.Robbin and D.Salamon, *Dynamical Systems, Shape Theory and the Conley Index*, Ergodic Th. Dyn. Sys. **8 Suppl** (1988), 375-393.

- [21] J.Rossignac and A.Szymczak, *Wrap&Zip: Linear Decoding of planar triangle graphs*, to appear in Computational Geometry: Theory & Applications.
- [22] D.Salamon, *Connected Simple Systems and the Conley Index of Isolated Invariant Sets*, Trans. AMS **291** (1985), 1–41.
- [23] A.W.Schurle, *Topics in Topology*, Elsevier North Holland, Inc. 1979.
- [24] E.Spanier, *Algebraic topology*, McGraw Hill 1966.
- [25] A.Szymczak, *The Conley index for discrete semidynamical systems*, Topology Appl. **66** (1995), 215-240.
- [26] A.Szymczak, *The Conley index and symbolic dynamics*, Topology 35 (1996), 287-299.
- [27] A.Szymczak, *The Conley index for decompositions of isolated invariant sets*, Fund. Math. **148** (1995), 71–90.
- [28] A.Szymczak, *A combinatorial procedure for finding isolating neighbourhoods and index pairs*, Proc. Royal Soc. Edinburgh **127A** (1997), 1075-1088.
- [29] A.Szymczak, *A cup product pairing and time-duality for discrete dynamical systems*, Topology **37** (1998), 1299–1311.
- [30] A.Szymczak and J.Rossignac, *Grow&Fold: Compression of Tetrahedral Meshes*, Solid Modeling'99.
- [31] A.Szymczak, K.Wójcik and P.Zgliczyński, *On the Conley index in the invariant subspace*, Topology Appl. **87** (1998), 105–115.